The Shifted Boundary Method:

A Framework for Embedded Computational Mechanics

Guglielmo Scovazzi, Alex Main, Nabil Atallah,
Ting Song, Kangan Li, Oriol Colomés-Gené,
Léo Nouveau, Mehdi Khalloufi (*Duke University*)

M. Ricchiuto (INRIA Bordeaux)

C. Canuto (*Politecnico di Torino*)

G. Rozza, G. Stabile, E. Karatzas (*SISSA, Trieste*)

ICIAM Conference, 2019, Valencia (Spain),

Thursday July 18, 2019

Duke UNIVERSITY

ICIAM 2019 VALENCIA

Motivation I

Complex geometry is still a key challenge in engineering simulations

- Engineering simulations are dominated by geometric complexity
- The merging of topology optimization and advanced manufacturing (e.g., *additive manufacturing*) exacerbates geometric complexity

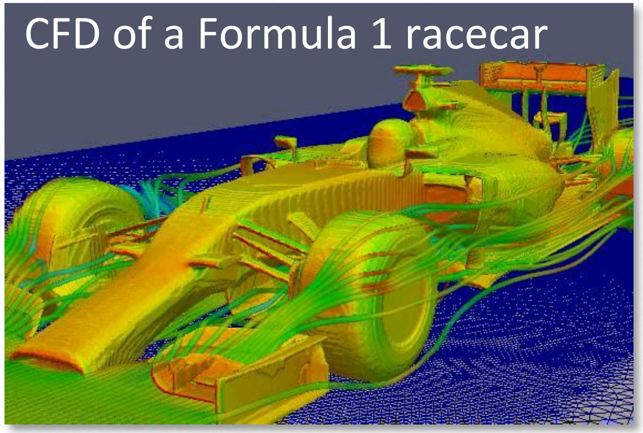
CFD of a Formula 1 racecar

Structural joint (welded)

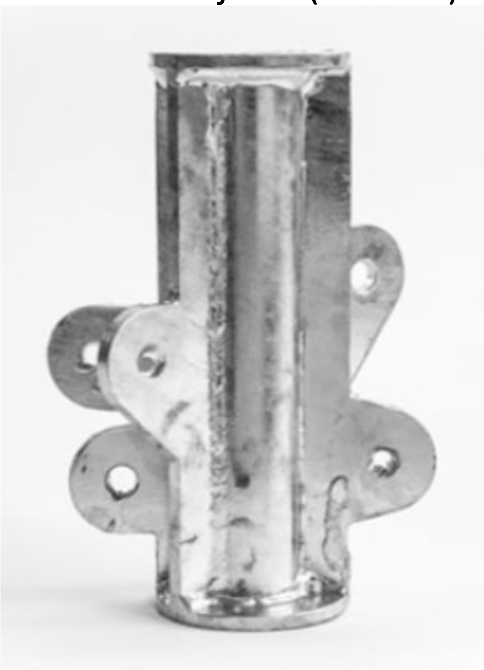

Structural joint (3D-printed)

Geometric model of a vascular stent

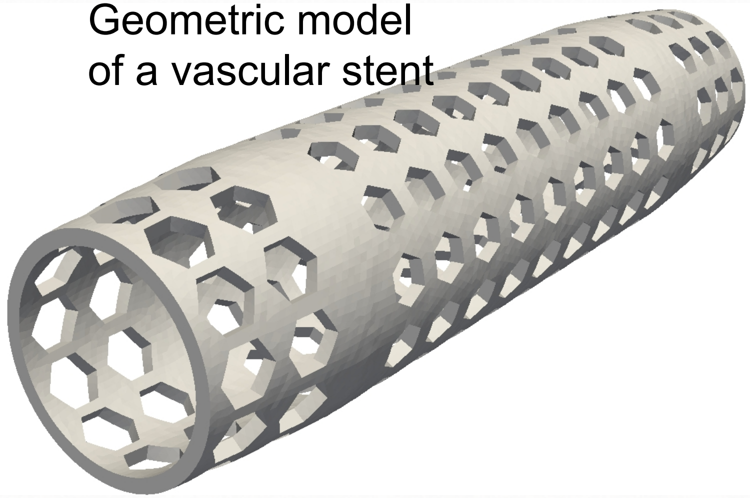

Motivation II

Imaging-to-computing, an *emerging* field:

An efficient transition from geometries reconstructed from images to computation may impact and transform many fields of application:

- *Biomedical engineering*: CT-scans are given as pixilated data or STL format (collections of triangular facets and their nodal coordinates). Body-fitted meshing can be quite hard to perform.
- *Subsurface imaging and computing* (meshing requires considerable effort in reservoir engineering applications)
- *Additive manufacturing simulations* (e.g., 3D-printing). The typical file format for 3D-printers is again STL

In these examples the geometric information is not very precise and/or consistent (surfaces with *gaps* and *overlaps*, typical of computer graphics, STL = set of disconnected triangular faces)

Overview

Two commonly used computational strategies:

1. *Body-fitted grids.* The grid conforms to the boundary geometry of the shape to be simulated.
   - *Advantages*: Easier treatment of the boundary conditions (and boundary layers)
   - *Limitations*: Requires more advanced meshing for complex geometry, or re-meshing in problems with large deformations

2. *Embedded/immersed grids*. The shape to be simulated is fully or partially embedded (or immersed) into a regular background grid.
   - *Advantages*: Generality of the method, especially if coupling heterogeneous computational frameworks, rapid prototyping
   - *Limitations*: More complex enforcement of boundary conditions

Existing Embedded Boundary Methods

Unfitted/Embedded Finite Element Methods

- Embedded methods of finite element type (a.k.a. *cutFEMs*, *unfitted FEMs, Finite Cell Method, Embedded Splines, IGA-Immersogeometric etc.*) often rely on XFEM methodologies to integrate on cut cells, *Inverse Lax-Wendroff procedure* (DG) [Burman, Hansbo, Larson, Massing, Cirak, Kamenski, Schillinger, Parvizian, Düster, Rank, Wall, Annavarapu, Dolbow, Harari, Moës, Badia, Rossi, C-W. Shu etc.]
- Unfitted/embedded FEMs typically utilize *Lagrange multipliers* or *Nitsche* variational formulations
- CutFEMs/unfitted FEMs require data structures and special quadratures to integrate on geometrically complex cut cells
- *The small cut-cell problem*: Integration over cut cells introduces additional interface degrees of freedom that may yield stability problems, very small time-steps or poor matrix conditioning. [Burman & Hansbo *Appl. Num. Math.* (2012)]. Solution: *ghost penalty*, and related methods

Overview of the Shifted Boundary Method

Key ideas:

- Use a *purely* embedded approach
- Use the Nitsche framework to impose boundary conditions weakly
- Apply boundary conditions on a surrogate boundary, near the true boundary
- Appropriately modify the boundary condition to account for the discrepancy between surrogate and true boundary

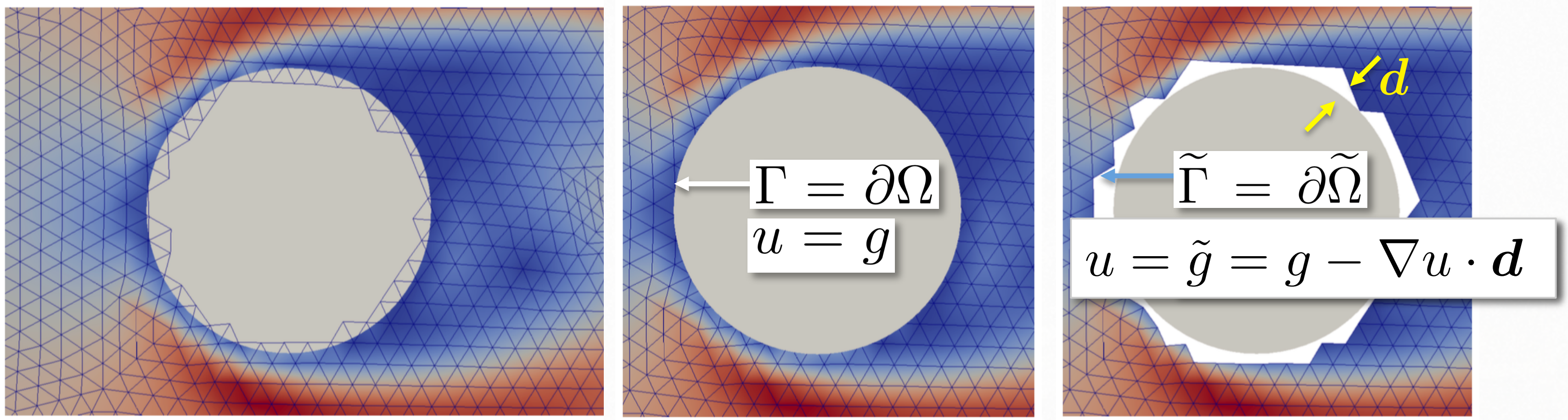

The Shifted Boundary Method: Key Ideas

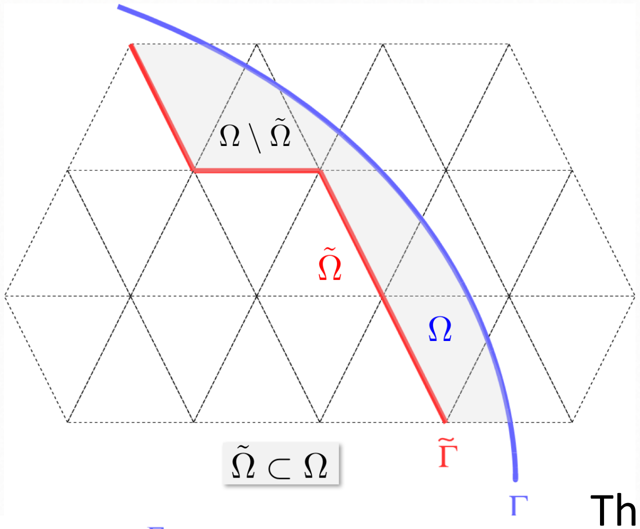

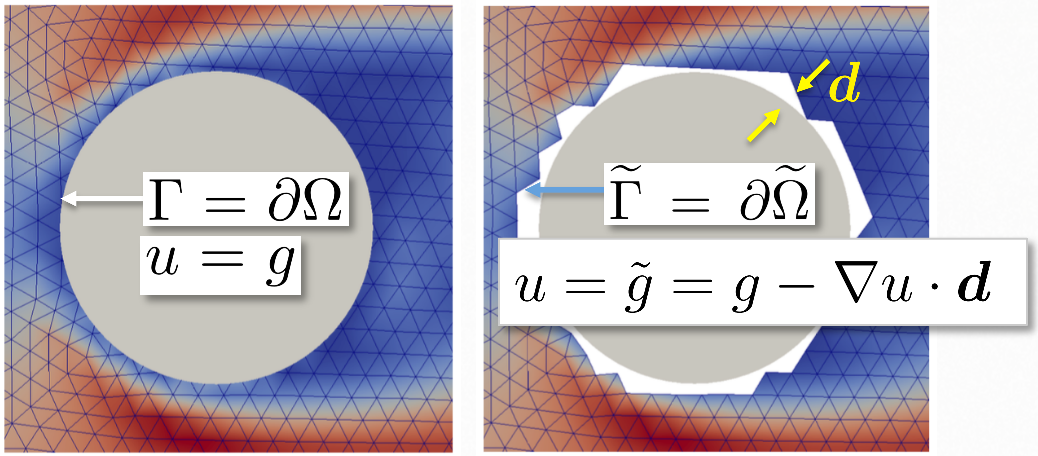

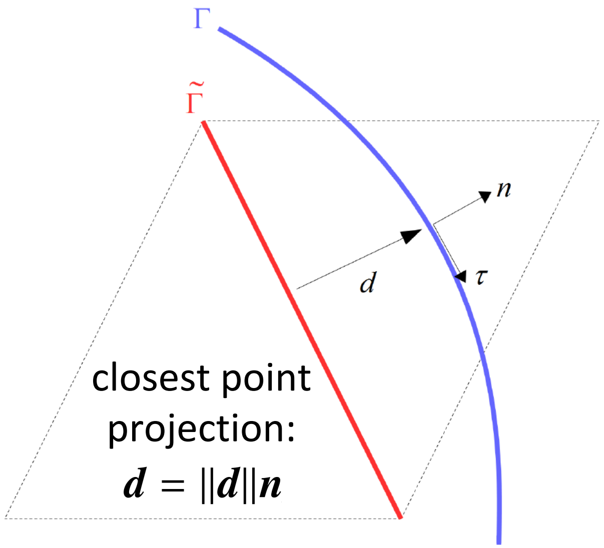

The extension map $\boldsymbol{M}$ & a distance vector function $\boldsymbol{d}$

$$\boldsymbol{M} : \tilde{\Gamma} \to \Gamma$$
$$\tilde{\boldsymbol{x}} \mapsto \boldsymbol{x}$$

$$\boldsymbol{d}_{\boldsymbol{M}}(\tilde{\boldsymbol{x}}) = \boldsymbol{x} - \tilde{\boldsymbol{x}} = [\,\boldsymbol{M} - \boldsymbol{I}\,](\tilde{\boldsymbol{x}})$$

Extension of functions defined on boundaries: $\bar{\psi}(\tilde{\boldsymbol{x}}) \equiv \psi(\boldsymbol{M}(\tilde{\boldsymbol{x}}))$

Important assumption (resolution): $\boldsymbol{n} \cdot \tilde{\boldsymbol{n}} > 0$

Surrogate domain geometric representation: via Physbam library (Fedkiw, Stanford U.), and the improved version developed in the Farhat research group (Stanford U.)

The (Base) Nitsche Method

A prototypical example: The Poisson problem

Strong form of the equation

$$\begin{aligned} \Delta u + f &= 0 \qquad \text{on } \Omega \\ u &= g \qquad \text{on } \Gamma = \partial\Omega \end{aligned}$$

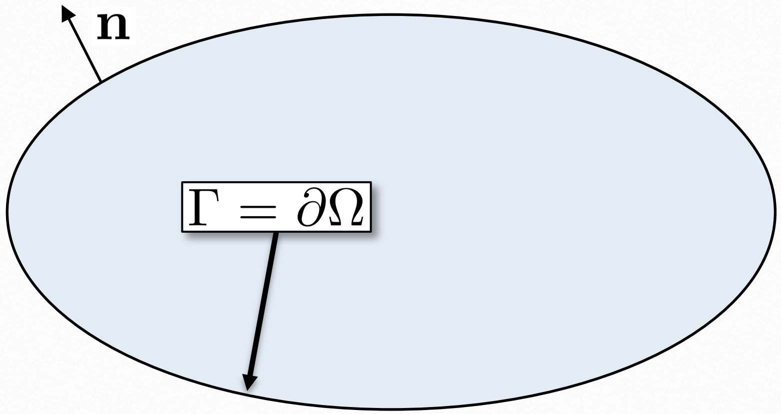

Weak form of the equation with weak boundary conditions (*Nitsche method*):

$$\int_\Omega w_{,i} u_{,i} \qquad\qquad = \int_\Omega w f$$

The Shifted Nitsche Method

A prototypical example: The Poisson problem

Weak form of the equation with weak boundary conditions (Nitsche method):

$$\int_{\Omega} w_{,i} u_{,i} - \int_{\Gamma} w u_{,i} n_i - \int_{\Gamma} w_{,i} (u - g) n_i + \alpha \int_{\Gamma} (u - g) w = \int_{\Omega} w f$$

Shifted Nitsche method:

$$\int_{\widetilde{\Omega}} w_{,i} u_{,i} - \int_{\widetilde{\Gamma}} w u_{,i} n_i - \int_{\widetilde{\Gamma}} w_{,i} (u - \widetilde{g}) n_i + \alpha \int_{\widetilde{\Gamma}} (u - \widetilde{g}) \widetilde{w} = \int_{\widetilde{\Omega}} w f$$

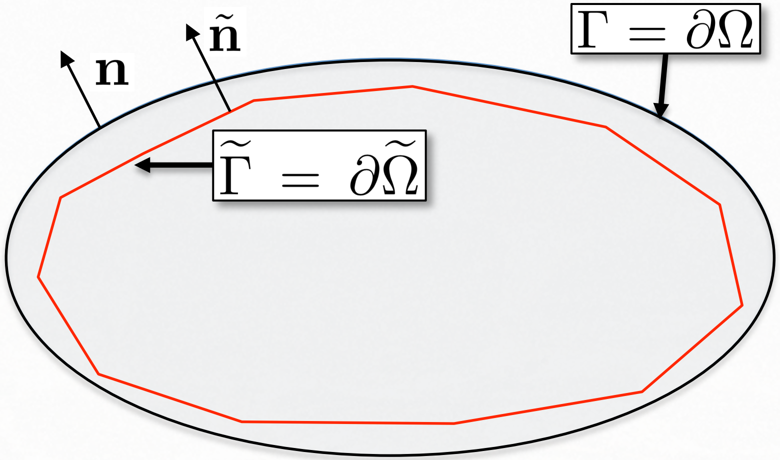

The Shifted Nitsche Method

A prototypical example: The Poisson problem

Weak form of the equation with weak boundary conditions (Nitsche method):

$$\int_{\widetilde{\Omega}} w_{,i} u_{,i} - \int_{\widetilde{\Gamma}} w u_{,i} n_i - \int_{\widetilde{\Gamma}} w_{,i} (u - \widetilde{g}) n_i + \alpha \int_{\widetilde{\Gamma}} (u - \widetilde{g}) \widetilde{w} = \int_{\widetilde{\Omega}} w f$$

$$\int_{\widetilde{\Omega}} w_{,i} u_{,i} - \int_{\widetilde{\Gamma}} w u_{,i} \tilde{n}_i - \int_{\widetilde{\Gamma}} w_{,i} (u + u_{,j} d_j - g) \tilde{n}_i + \alpha \int_{\widetilde{\Gamma}} (u + u_{,j} d_j - g)(w + w_{,k} d_k) = \int_{\widetilde{\Omega}} w f$$

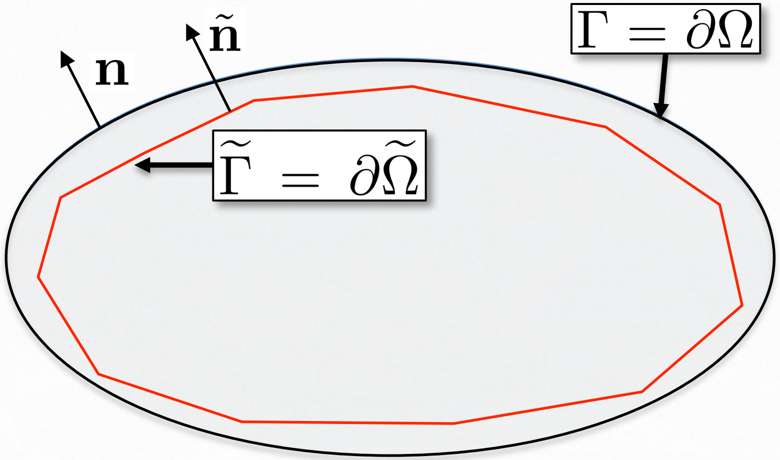

Numerical Results: Poisson Problem

Numerical convergence test with an exact solution

$$\Delta u + 1 = 0 \qquad on\ \Omega$$

$$u|_{\Gamma} = 0$$

Exact solution:

$$u = \frac{1}{4}(R^2 - r^2)$$

Convergence of the L^2 norm of the error

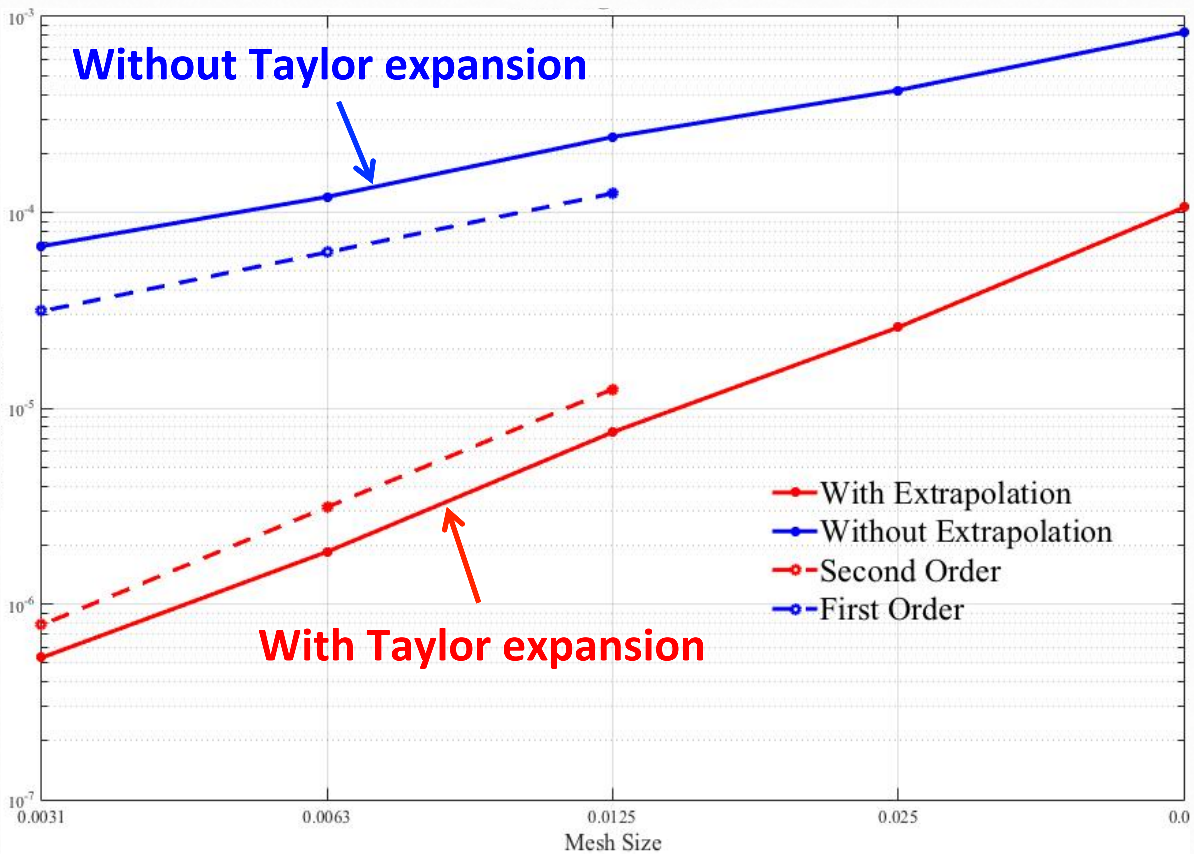

Numerical Results: Poisson Problem

Condition number trends

For the previous problem, the algebraic condition number has the following properties:

- About 3 times larger than for the body-fitted method
- Same scaling with h^{-2} has for the body-fitted method

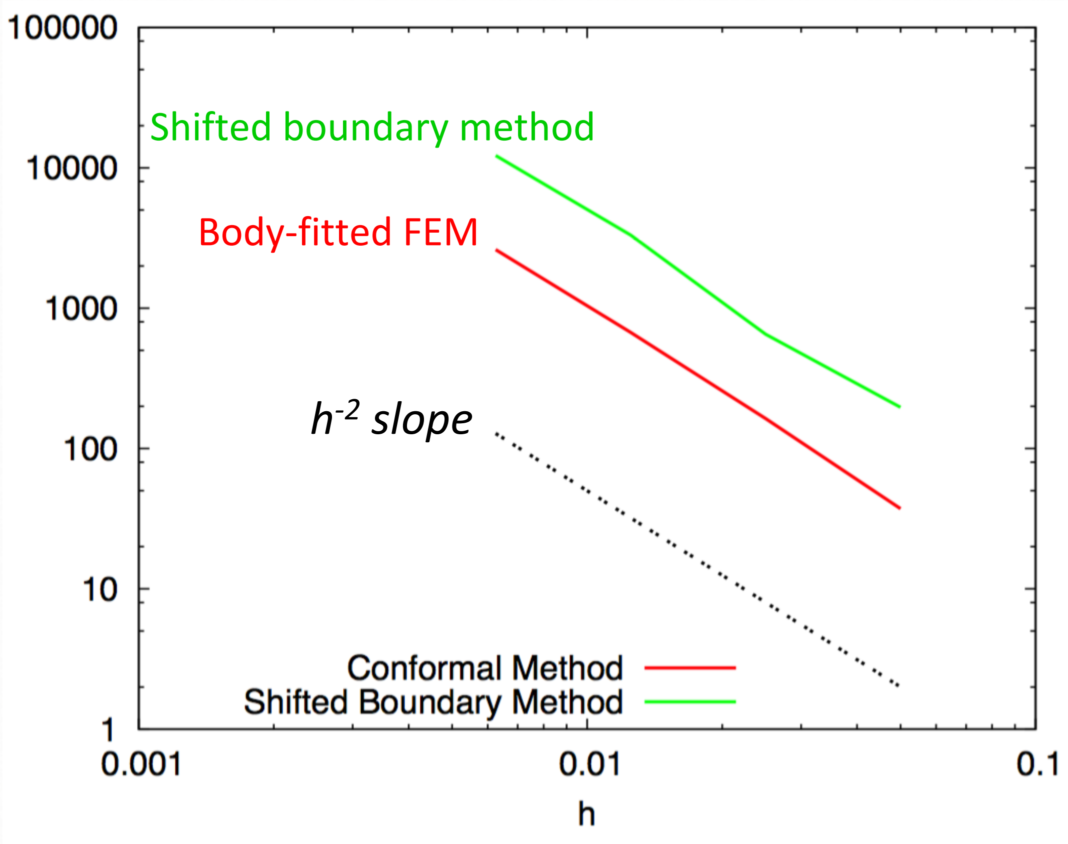

Numerical Analysis: Poisson Problem

Coercivity of the SBM variational form (sketch of proof for Poisson operator)

$$
\begin{aligned}
a_u^h(u^h, w^h) &= l_u^h(w^h) \\
a_u^h(u^h, w^h) &= (\nabla w^h, \nabla u^h)_{\tilde{\Omega}} - \langle w^h + \nabla w^h \cdot \boldsymbol{d}, \nabla u^h \cdot \tilde{\boldsymbol{n}} \rangle_{\tilde{\Gamma}_D} - \langle \nabla w^h \cdot \tilde{\boldsymbol{n}}, u^h + \nabla u^h \cdot \boldsymbol{d} \rangle_{\tilde{\Gamma}_D} + \langle \nabla w^h \cdot \boldsymbol{d}, \nabla u^h \cdot \tilde{\boldsymbol{n}} \rangle_{\tilde{\Gamma}_D} \\
&\quad + \langle \alpha / h^{\perp} \, (w^h + \nabla w^h \cdot \boldsymbol{d}), u^h + \nabla u^h \cdot \boldsymbol{d} \rangle_{\tilde{\Gamma}_D} + \langle \beta \, \|\boldsymbol{d}\| \, w^h_{,\tilde{\tau}_i}, u^h_{,\tilde{\tau}_i} \rangle_{\tilde{\Gamma}_D} \\
l_u^h(w^h) &= (w^h, f)_{\tilde{\Omega}} - \langle \nabla w^h \cdot \tilde{\boldsymbol{n}}, \bar{u}_D \rangle_{\tilde{\Gamma}_D} + \langle \alpha / h^{\perp} \, (w^h + \nabla w^h \cdot \boldsymbol{d}), \bar{u}_D \rangle_{\tilde{\Gamma}_D} + \langle \beta \, \|\boldsymbol{d}\| \, w^h_{,\tilde{\tau}_i}, \bar{u}_{D,\tilde{\tau}_i} \rangle_{\tilde{\Gamma}_D} \, .
\end{aligned}
$$

… and replace $w^h = u^h$:

$$
\begin{aligned}
a_u^h(u^h, u^h) = \; & \|\nabla u^h\|^2_{0,\tilde{\Omega}} - 2\langle u^h + \nabla u^h \cdot \boldsymbol{d}, \nabla u^h \cdot \tilde{\boldsymbol{n}} \rangle_{\tilde{\Gamma}_D} + \langle \nabla u^h \cdot \boldsymbol{d}, \nabla u^h \cdot \tilde{\boldsymbol{n}} \rangle_{\tilde{\Gamma}_D} \\
& + \alpha \, \| \sqrt{1/h^{\perp}} \, (u^h + \nabla u^h \cdot \boldsymbol{d}) \|^2_{0,\tilde{\Gamma}_D} + \beta \, \| \sqrt{h^{\perp}} \, u^h_{,\tilde{\tau}} \|^2_{0,\tilde{\Gamma}_D} \, ,
\end{aligned}
$$

Use the following decomposition

$$
\begin{aligned}
\nabla u^h \cdot \tilde{\boldsymbol{n}} &= \left((\nabla u^h \cdot \boldsymbol{n}) \boldsymbol{n} + (\nabla u^h \cdot \boldsymbol{\tau}_i) \boldsymbol{\tau}_i \right) \cdot \tilde{\boldsymbol{n}} \, , \\
\nabla u^h \cdot \boldsymbol{d} &= \nabla u^h \cdot \boldsymbol{n} \, \|\boldsymbol{d}\| \, .
\end{aligned}
$$

Numerical Analysis: Poisson Problem

… sketch of coercivity proof continued

$$\langle \nabla u^h \cdot \boldsymbol{d}, \nabla u^h \cdot \tilde{\boldsymbol{n}} \rangle_{\tilde{\Gamma}_D} \geq \| \sqrt{(\boldsymbol{n} \cdot \tilde{\boldsymbol{n}}) \, \|\boldsymbol{d}\|} \, \nabla u^h \cdot \boldsymbol{n} \|^2_{0,\tilde{\Gamma}_D} - |\langle (\partial_n u^h \; \boldsymbol{n}) \cdot \boldsymbol{d}, (\partial_{\tau_j} u^h \; \boldsymbol{\tau}_j) \cdot \tilde{\boldsymbol{n}} \rangle_{\tilde{\Gamma}_D}|$$

$$\geq \| \sqrt{(\boldsymbol{n} \cdot \tilde{\boldsymbol{n}}) \, \|\boldsymbol{d}\|} \, \nabla u^h \cdot \boldsymbol{n} \|^2_{0,\tilde{\Gamma}_D} - \| \sqrt{\|\boldsymbol{d}\|} \, \partial_n u^h \|_{0,\tilde{\Gamma}_D} \| \sqrt{\|\boldsymbol{d}\|} \, u^h_{,\bar{\tau}} \|_{0,\tilde{\Gamma}_D}$$

$$\geq \| \sqrt{(\boldsymbol{n} \cdot \tilde{\boldsymbol{n}}) \, \|\boldsymbol{d}\|} \, \nabla u^h \cdot \boldsymbol{n} \|^2_{0,\tilde{\Gamma}_D} - \left(\frac{\epsilon_1}{2} \| \sqrt{\|\boldsymbol{d}\|} \, \nabla u^h \cdot \boldsymbol{n} \|^2_{0,\tilde{\Gamma}_D} + \frac{1}{2\epsilon_1} \| \sqrt{\|\boldsymbol{d}\|} \, u^h_{,\bar{\tau}} \|^2_{0,\tilde{\Gamma}_D} \right)$$

and

$$2\langle u^h + \nabla u^h \cdot \boldsymbol{d}, \nabla u^h \cdot \tilde{\boldsymbol{n}} \rangle_{\tilde{\Gamma}_D} \leq \frac{1}{\epsilon} \| \sqrt{1/h^\perp} \, (u^h + \nabla u^h \cdot \boldsymbol{d}) \|^2_{0,\tilde{\Gamma}_D} + \epsilon \| \sqrt{h^\perp} \, \nabla u^h \cdot \tilde{\boldsymbol{n}} \|^2_{0,\tilde{\Gamma}_D}$$

In conclusion:

$$|||u^h|||^2_{\mathrm{SB_u}} = \|\nabla u^h\|^2_{0,\tilde{\Omega}} + \| \sqrt{(\boldsymbol{n} \cdot \tilde{\boldsymbol{n}}) \, \|\boldsymbol{d}\|} \, \nabla u^h \cdot \boldsymbol{n} \|^2_{0,\tilde{\Gamma}_D} + \| \sqrt{1/h^\perp} \, (u^h + \nabla u^h \cdot \boldsymbol{d}) \|^2_{0,\tilde{\Gamma}_D} + \left\| \sqrt{\|\boldsymbol{d}\|} \, u^h_{,\bar{\tau}} \right\|^2_{0,\tilde{\Gamma}_D} ,$$

$$C_{\mathrm{SB_u}} = \min\left(1 - C_I \left(\epsilon + \frac{\epsilon_1}{2} \right), \alpha - \frac{1}{\epsilon}, \beta - \frac{1}{2\epsilon_1} \right) .$$

Numerical Analysis: Poisson Problem

Sketch of the proof of convergence

Estimate the consistency error:

$$a_u^h(u, w^h) - l_u^h(w^h) = \underbrace{\tilde{a}^h(u, w^h) - \tilde{l}^h(w^h)}_{=0} - \langle \sqrt{h^\perp}\, \nabla w^h \cdot \tilde{\boldsymbol{n}},\ \sqrt{1/h^\perp}\, \underbrace{(u + \nabla u \cdot \boldsymbol{d} - \bar{u}_D)}_{O(h^2)} \rangle_{\tilde{\Gamma}_D}$$

$$+ \langle \alpha \sqrt{1/h^\perp}\, (w^h + \nabla w^h \cdot \boldsymbol{d}),\ \sqrt{1/h^\perp}\, \underbrace{(u + \nabla u \cdot \boldsymbol{d} - \bar{u}_D)}_{O(h^2)} \rangle_{\tilde{\Gamma}_D} + \langle \beta \sqrt{\|\boldsymbol{d}\|}\, w^h_{,\tilde{\tau}_i},\ \underbrace{\sqrt{\|\boldsymbol{d}\|}\, (u_{,\tilde{\tau}_i} - \bar{u}_{D,\tilde{\tau}_i})}_{O(h^{3/2})} \rangle_{\tilde{\Gamma}_D}$$

$$\leq \boxed{|||w^h|||_{\mathrm{SB_u}}\, O\left(h^{3/2}\right)} \,,$$

Apply second Strang's lemma:

$$|||u - u^h|||_{\mathrm{SB_u}} \leq \|u - u^h\|_{V(h)}$$

$$\leq \left(1 + \frac{\|a_u^h\|_{V(h)\times V^h(\tilde{\Omega})}}{C_{\mathrm{SB}_u}}\right) \underbrace{\inf_{w^h \in V^h(\tilde{\Omega})} \|u - w^h\|_{V(h)}}_{O(h)} + \underbrace{\frac{1}{C_{\mathrm{SB_u}}} \sup_{v^h \in V^h(\tilde{\Omega})} \frac{\boxed{|l^h(v^h) - a_u^h(u, v^h)|}}{|||v^h|||_{\mathrm{SB_u}}}}_{O(h^{3/2})}$$

Continuity/boundedness

Coercivity

$$\leq Ch \,,$$

Numerical Analysis: Poisson Problem

Sketch of (duality) L²-estimates [a new/harder version of Nitsche-Aubin trick]

$$a_u^h(u,w) = a_{s;c}^h(u,w) + a_{s;d}^h(u,w) + a_{u;d}^h(u,w)\ ,$$

$$a_{s;c}^h(u,w) = (\nabla w\,,\nabla u)_{\tilde\Omega} - \langle w\,,\nabla u\cdot\tilde{\boldsymbol n}\rangle_{\tilde\Gamma_D} - \langle \nabla w\cdot\tilde{\boldsymbol n}\,,\,u\rangle_{\tilde\Gamma_D} + \langle \alpha/h^{\perp} w\,,\,u\rangle_{\tilde\Gamma_{\tilde\Gamma_D}}\ ,$$ (Body-fitted)

$$a_{s;d}^h(u,w) = -\langle \nabla w\cdot\boldsymbol d,\nabla u\cdot\tilde{\boldsymbol n}\rangle_{\tilde\Gamma_D} - \langle \nabla w\cdot\tilde{\boldsymbol n},\nabla u\cdot\boldsymbol d\rangle_{\tilde\Gamma_D} + \langle \alpha/h^{\perp}\,\nabla w\cdot\boldsymbol d,u\rangle_{\tilde\Gamma_D} + \langle \alpha/h^{\perp}\,w,\nabla u\cdot\boldsymbol d\rangle_{\tilde\Gamma_D}$$
$$+\ \langle \beta\,\|\boldsymbol d\|\,w_{,\tilde\tau_i},u_{,\tilde\tau_i}\rangle_{\tilde\Gamma_D} + \langle \alpha/h^{\perp}\,\nabla w\cdot\boldsymbol d,\nabla u\cdot\boldsymbol d\rangle_{\tilde\Gamma_D}\ ,$$ (SBM-term, symmetric)

$$a_{u;d}^h(u,w) = \langle \nabla w\cdot\boldsymbol d,\nabla u\cdot\tilde{\boldsymbol n}\rangle_{\tilde\Gamma_D}\ .$$ (SBM-term, unsymmetric)

SBM terms

$$\begin{cases} -\Delta\psi = u-u^h\,, & \text{in } \tilde\Omega\,,\\ \psi = 0\,, & \text{in } \tilde\Gamma = \partial\tilde\Omega\,. \end{cases}$$ (Auxiliary (dual/adjoint) problem)

$$a_{s;c}^h(w,\psi) = a_u^h(w,\psi) - a_{s;d}^h(w,\psi) - a_{u;d}^h(w,\psi) = (w\,,\,u-u^h)_{\tilde\Omega}\ ,$$ (Weak dual problem)

Taking $w = u - u^h$, we obtain:

$$\|u-u^h\|_{0;\tilde\Omega}^2 = a_u^h(u-u^h,\psi-\psi_I) + a_u^h(u-u^h,\psi_I) + R_c(u-u^h,\psi)\ ,$$

Numerical Analysis: Poisson Problem

Sketch of (duality) L²-estimates [a new/harder version of Nitsche-Aubin trick]

$$\|u - u^h\|^2_{0;\tilde{\Omega}} = a^h_u(u - u^h, \psi - \psi_I) + a^h_u(u - u^h, \psi_I) + R_c(u - u^h, \psi) ,$$

Every term can be bounded:

$$a^h_u(u - u^h, \psi - \psi_I) \leq C_{b_u} |||u - u^h|||_{\mathrm{SB_s}} |||\psi - \psi_I|||_{\mathrm{SB_s}} \leq C_{b_u} C_{int} \|u - u^h\|_{V_s(h)} h |\psi|_{2;\tilde{\Omega}} ,$$

$$\begin{aligned} a^h_u(u - u^h, \psi_I) &= a^h_u(u, \psi_I) - l^h_u(\psi_I) \\ &= \langle \alpha/h^\perp \nabla\psi_I \cdot \boldsymbol{d} - \nabla\psi_I \cdot \tilde{\boldsymbol{n}}, \underbrace{u + \nabla u \cdot \boldsymbol{d} - \bar{u}_D}_{O(h^2)} \rangle_{\tilde{\Gamma}_D} + \langle \beta\, \psi_{I,\bar{\tau}_i}, \underbrace{\|\boldsymbol{d}\| \, (u_{,\bar{\tau}_i} - \bar{u}_{D,\bar{\tau}_i})}_{O(h^2)} \rangle_{\tilde{\Gamma}_D} \\ &\leq C'_{int} |\psi|_{2;\tilde{\Omega}} O\left(h^2\right) , \end{aligned}$$

$$\begin{aligned} R_c(\psi, u - u^h) = & \langle \sqrt{\|\boldsymbol{d}\|/(\boldsymbol{n} \cdot \tilde{\boldsymbol{n}})} \nabla\psi \cdot \tilde{\boldsymbol{n}}, \sqrt{(\boldsymbol{n} \cdot \tilde{\boldsymbol{n}}) \|\boldsymbol{d}\|} \nabla(u - u^h) \cdot \boldsymbol{n} \rangle_{\tilde{\Gamma}_D} \\ & - \langle \sqrt{\alpha/h^\perp} \nabla\psi \cdot \boldsymbol{d}, \sqrt{\alpha/h^\perp} (u - u^h + \nabla(u - u^h) \cdot \boldsymbol{d}) \rangle_{\tilde{\Gamma}_D} \\ & + \langle \sqrt{\beta \|\boldsymbol{d}\|} \psi_{,\bar{\tau}_i}, \sqrt{\beta \|\boldsymbol{d}\|} (u - u^h)_{,\bar{\tau}_i} \rangle_{\tilde{\Gamma}_D} \\ \leq & C_{\tilde{\Gamma}} |||u - u^h|||_{\mathrm{SB_s}} h^{1/2} |\psi|_{2;\tilde{\Omega}} . \end{aligned}$$

Finally:

$$\boxed{\|u - u^h\|_{0;\tilde{\Omega}} \leq C_{NA} h^{3/2}}$$

(Possibly, this estimate is not sharp, since, numerically, we observe second order!)

Numerical Analysis: Stokes Flow Problem

[Collaboration with Claudio Canuto, Mathematics Dept., Politecnico di Torino]

Stability (LBB)

$$\mathscr{B}([\boldsymbol{u}^h, p^h]; [\boldsymbol{w}^h, q^h]) \geq \alpha_{LBB} \, ||[\boldsymbol{u}^h, p^h]\,||_{\mathscr{B}} \, ||[\boldsymbol{w}^h, q^h]\,||_{\mathscr{B}}$$

An LBB *inf-sup* condition can be derived in the case of the Stokes' operator

Convergence (in natural norm)

$$||\,[\boldsymbol{u}, p] - [\boldsymbol{u}^h, p^h]\,||_{\boldsymbol{W}(\tilde{\Omega};h)} \leq C\, h_{\tilde{\Omega}} \left(||\nabla(\nabla \boldsymbol{u})||_{0,\Omega} + ||\nabla p||_{0,\tilde{\Omega}} \right)$$

The proof is analogous to the one for the Poisson problem, using the *inf-sup* LBB condition and Strang's second lemma.

Duality estimates (L^2-estimates for the velocity field)

$$||\boldsymbol{u} - \boldsymbol{u}^h||_{0;\tilde{\Omega}} \leq C_0\, h_{\tilde{\Omega}}^{3/2} \left(||\nabla(\nabla \boldsymbol{u})||_{0,\tilde{\Omega}} + ||\nabla p||_{0,\tilde{\Omega}} \right)$$

Analogous but more complicated proof than in the Poisson case. We observe quadratic convergence for the velocity, in practical calculations

Advection-Diffusion Problem

Strong form of the equations

$$
\begin{aligned}
\nabla \cdot (\boldsymbol{a}u - \kappa \nabla u) &= f, && \text{on } \Omega, \\
u &= g, && \text{on } \Gamma, \\
-(\boldsymbol{a}u - \kappa \nabla u) \cdot \boldsymbol{n} &= h, && \text{on } \Gamma_h^-, \\
\kappa \nabla u \cdot \boldsymbol{n} &= h, && \text{on } \Gamma_h^+,
\end{aligned}
$$

$\boldsymbol{a}$ is a solenoidal vector field ($\nabla \cdot \boldsymbol{a} = 0$)

$$\boldsymbol{a} \cdot \nabla u - \kappa \Delta u = f$$

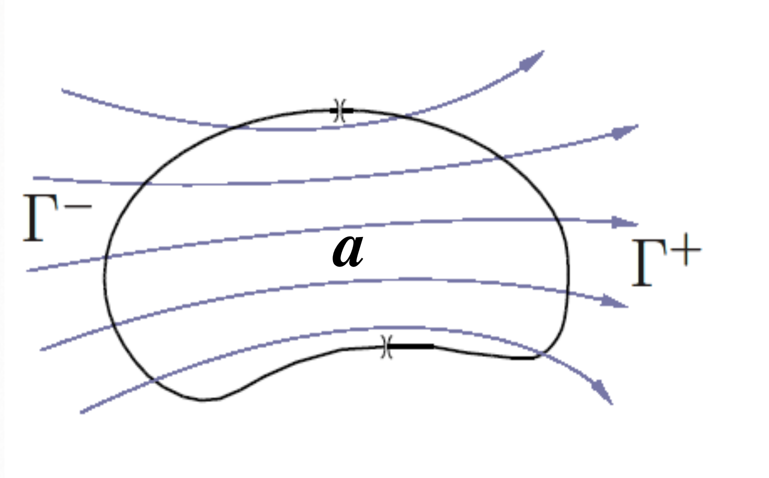

$$\Gamma_g^- = \{\boldsymbol{x} \in \Gamma_g \mid \boldsymbol{a} \cdot \boldsymbol{n} < 0\}$$

$$\Gamma_h^- = \{\boldsymbol{x} \in \Gamma_h \mid \boldsymbol{a} \cdot \boldsymbol{n} < 0\}$$

$$\Gamma_g^+ = \Gamma_g \setminus \Gamma_g^-$$

$$\Gamma_h^+ = \Gamma_h \setminus \Gamma_h^-$$

Numerical Analysis: Advection-Diffusion

Variational formulation (shifted Nitsche-type + SUPG)

Find $u^h \in V^h(\tilde{\Omega})$ *such that,* $\forall w^h \in V^h(\tilde{\Omega})$,

$$a^h(u^h, w^h) = l^h(w^h)\,,$$

$$\begin{aligned}a^h(u^h, w^h) = &-(\nabla w^h, \boldsymbol{a} u^h)_{\tilde{\Omega}} + (\nabla w^h, \kappa \nabla u^h)_{\tilde{\Omega}} + (\tau\, \boldsymbol{a} \cdot \nabla w^h, \boldsymbol{a} \cdot \nabla u^h - \kappa \Delta u^h)_{\tilde{\Omega}'} \\ &+ \langle w^h, u^h\, \boldsymbol{a} \cdot \tilde{\boldsymbol{n}} \rangle_{\tilde{\Gamma}^+} - \langle w^h, \kappa \nabla u^h \cdot \tilde{\boldsymbol{n}} \rangle_{\tilde{\Gamma}_D} - \langle \kappa \nabla w^h \cdot \tilde{\boldsymbol{n}}, u^h + \nabla u^h \cdot \boldsymbol{d} \rangle_{\tilde{\Gamma}_D^+} - \langle \kappa \nabla w^h \cdot \tilde{\boldsymbol{n}}, u^h \rangle_{\tilde{\Gamma}_D^-} \\ &+ \langle \alpha\, \kappa / h^{\perp}\, w^h, u^h \rangle_{\tilde{\Gamma}_D^-} + \langle \alpha\, \kappa / h^{\perp}\, (w^h + \nabla w^h \cdot \boldsymbol{d}), u^h + \nabla u^h \cdot \boldsymbol{d} \rangle_{\tilde{\Gamma}_D^+} + \langle \beta\, \kappa\, h^{\perp}\, w^h_{,\tilde{\tau}_i}, u^h_{,\tilde{\tau}_i} \rangle_{\tilde{\Gamma}_D^+}\,,\end{aligned}$$

$$\begin{aligned}l^h(w^h) = &\,(w^h, f)_{\tilde{\Omega}} + (\tau\, \boldsymbol{a} \cdot \nabla w^h, f)_{\tilde{\Omega}'} \\ &+ \langle w^h, t_N \rangle_{\tilde{\Gamma}_N} - \langle \kappa \nabla w^h \cdot \tilde{\boldsymbol{n}}, u_D \rangle_{\tilde{\Gamma}_D} - \langle w^h, u_D\, \boldsymbol{a} \cdot \tilde{\boldsymbol{n}} \rangle_{\tilde{\Gamma}_D^-} \\ &+ \langle \alpha\, \kappa / h^{\perp}\, w^h, u_D \rangle_{\tilde{\Gamma}_D^-} + \langle \alpha\, \kappa / h^{\perp}\, (w^h + \nabla w^h \cdot \boldsymbol{d}), u_D \rangle_{\tilde{\Gamma}_D^+} + \langle \beta\, \kappa\, h^{\perp}\, w^h_{,\tilde{\tau}_i}, \bar{u}_{D,\tilde{\tau}_i} \rangle_{\tilde{\Gamma}_D^+}\,.\end{aligned}$$

Conservation statement (selecting a constant test function)

(Dirichlet outflow)

$$\langle 1, u_D\, \boldsymbol{a} \cdot \tilde{\boldsymbol{n}} - \kappa \nabla u^h \cdot \tilde{\boldsymbol{n}} + \alpha\, \kappa / h^{\perp}\, (u^h - u_D) \rangle_{\tilde{\Gamma}_D^-} + \langle 1, u^h \boldsymbol{a} \cdot \tilde{\boldsymbol{n}} - \kappa \nabla u^h \cdot \tilde{\boldsymbol{n}} + \alpha\, \kappa / h^{\perp}\, (u^h - u_D) \rangle_{\tilde{\Gamma}_D^+}$$

(Dirichlet inflow) (Neumann inflow)

$$- \langle 1, t_N \rangle_{\tilde{\Gamma}_N^-} + \langle 1, u^h\, \boldsymbol{a} \cdot \tilde{\boldsymbol{n}} - t_N \rangle_{\tilde{\Gamma}_N^+} = (1, f)_{\tilde{\Omega}}$$

(Neumann outflow)

Numerical Analysis: Advection-Diffusion

Stability

$$a^h(u^h, u^h) \geq C_{\mathrm{SB}} |||u^h|||^2_{\mathrm{SB}} \,,$$

$$|||u^h|||^2_{\mathrm{SB}} = \| \, |\boldsymbol{a} \cdot \tilde{\boldsymbol{n}}|^{1/2} \, u^h \, \|_{0,\tilde{\Gamma}} + \kappa \, \|\nabla u^h\|^2_{0,\tilde{\Omega}} + \|\tau^{1/2} \, \boldsymbol{a} \cdot \nabla u^h\|^2_{0,\tilde{\Omega}}$$
$$+ \kappa \, \| \sqrt{1/h^{\perp}} \, u^h \, \|^2_{0,\tilde{\Gamma}^-_D} + \kappa \, \| \sqrt{1/h^{\perp}} \, (u^h + \nabla u^h \cdot \boldsymbol{d}) \, \|^2_{0,\tilde{\Gamma}^+_D} + \kappa \, \| \sqrt{h^{\perp}} \, u^h_{,\bar{\tau}_i} \|^2_{0,\tilde{\Gamma}_D} \,,$$

$$C_{\mathrm{SB}} = \min\left(\frac{1}{2} - C_I \left(2\epsilon_1 + \frac{\epsilon_2}{2} \right), \, \alpha - \frac{1}{\epsilon_1}, \, \beta - \frac{1}{2\epsilon_2} \right) .$$

Convergence

Analogous to the one for the Poisson problem, using again Strang's second lemma.

Incompressible Navier-Stokes Equations

Strong form

$$
\begin{aligned}
\rho(\boldsymbol{u}_{,t} + \boldsymbol{u}\cdot\nabla\boldsymbol{u}) + \nabla p - \nabla\cdot(2\mu\,\boldsymbol{\epsilon}(\boldsymbol{u})) - \rho\boldsymbol{b} &= 0\,, & \forall\boldsymbol{x}\in\Omega\,,\\
\nabla\cdot\boldsymbol{u} &= 0\,, & \forall\boldsymbol{x}\in\Omega\,,\\
\boldsymbol{u} &= \boldsymbol{g}\,, & \forall\boldsymbol{x}\text{ on }\Gamma_g\,,\\
-(\rho\boldsymbol{u}\otimes\boldsymbol{u}\,\chi_{\Gamma_h^-} + p\boldsymbol{I} - 2\mu\,\boldsymbol{\epsilon}(\boldsymbol{u}))\,\boldsymbol{n} &= \boldsymbol{h}\,, & \forall\boldsymbol{x}\text{ on }\Gamma_h\,.
\end{aligned}
$$

$$
\begin{aligned}
\Gamma_g^- &= \{\boldsymbol{x}\in\Gamma_g\,|\,\boldsymbol{g}\cdot\boldsymbol{n}<0\}\,,\\
\Gamma_h^- &= \{\boldsymbol{x}\in\Gamma_h\,|\,\boldsymbol{u}\cdot\boldsymbol{n}<0\}\,,\\
\Gamma_g^+ = \Gamma_g\setminus\Gamma_g^- &\text{ and } \Gamma_h^+ = \Gamma_g\setminus\Gamma_h^-
\end{aligned}
$$

Shifted boundary method (+ SUPG/PSPG/VMS stabilization)

Find $\boldsymbol{u}\in\boldsymbol{V}^h(\tilde{\Omega})$ *and* $p\in Q^h(\tilde{\Omega})$ *such that,* $\forall\boldsymbol{u}\in\boldsymbol{V}^h(\tilde{\Omega})$ *and* $\forall q\in Q^h(\tilde{\Omega})$,

$$
\begin{aligned}
0 =\;& \mathbb{NS}[\mu](\boldsymbol{u},p;\boldsymbol{w},q)\\
=\;& (\boldsymbol{w}\,,\rho\,(\boldsymbol{u}_{,t}+\boldsymbol{u}\cdot\nabla\boldsymbol{u}-\boldsymbol{b}))_{\tilde{\Omega}} - \langle\boldsymbol{w}\,,\rho\boldsymbol{u}\cdot\tilde{\boldsymbol{n}}\,(\boldsymbol{u}-\boldsymbol{g})\rangle_{\tilde{\Gamma}_g^-} - \langle\boldsymbol{w},\boldsymbol{h}\rangle_{\tilde{\Gamma}_h} - \langle\boldsymbol{w},\,(\boldsymbol{u}\cdot\tilde{\boldsymbol{n}})\,\rho\boldsymbol{u}\,\rangle_{\tilde{\Gamma}_h^-} - (\nabla\cdot\boldsymbol{w},p)_{\tilde{\Omega}} - (q,\nabla\cdot\boldsymbol{u})_{\tilde{\Omega}}\\
&+ (\boldsymbol{\epsilon}(\boldsymbol{w}),2\mu\,\boldsymbol{\epsilon}(\boldsymbol{u}))_{\tilde{\Omega}} - \langle\boldsymbol{w}\otimes\tilde{\boldsymbol{n}},2\mu\,\boldsymbol{\epsilon}(\boldsymbol{u})-p\boldsymbol{I}\rangle_{\tilde{\Gamma}_g} - \langle 2\mu\,\boldsymbol{\epsilon}(\boldsymbol{w}),\boxed{(\boldsymbol{u}+\chi_{\tilde{\Gamma}_g^+}(\nabla\boldsymbol{u})\boldsymbol{d}-\boldsymbol{g})}\otimes\tilde{\boldsymbol{n}}\rangle_{\tilde{\Gamma}_g}\\
&+ \langle\,\boldsymbol{w}+\chi_{\tilde{\Gamma}_g^+}(\nabla\boldsymbol{w})\boldsymbol{d}\,,\,\mu/h\,(\alpha_1\boldsymbol{I}+\alpha_2\,\mathrm{Re}[\mu]\,\boldsymbol{n}\otimes\boldsymbol{n})\,\boxed{(\boldsymbol{u}+\chi_{\tilde{\Gamma}_g^+}(\nabla\boldsymbol{u})\boldsymbol{d}-\boldsymbol{g})}\rangle_{\tilde{\Gamma}_g}\\
&\boxed{+\,\beta\,\langle\,\nabla_{\tilde{\tau}_i}\boldsymbol{w},\,2\mu\,h\,(\nabla_{\tilde{\tau}_i}\boldsymbol{u}-\nabla_{\tilde{\tau}_i}\bar{\boldsymbol{g}})\,\rangle_{\tilde{\Gamma}_g}}\,.
\end{aligned}
$$

Euler-Lagrange and conservation statements analogous to the advection-diffusion case

Duke UNIVERSITY

The Shifted Boundary Method

Convergence test (Navier-Stokes): Decelerating cylinder test

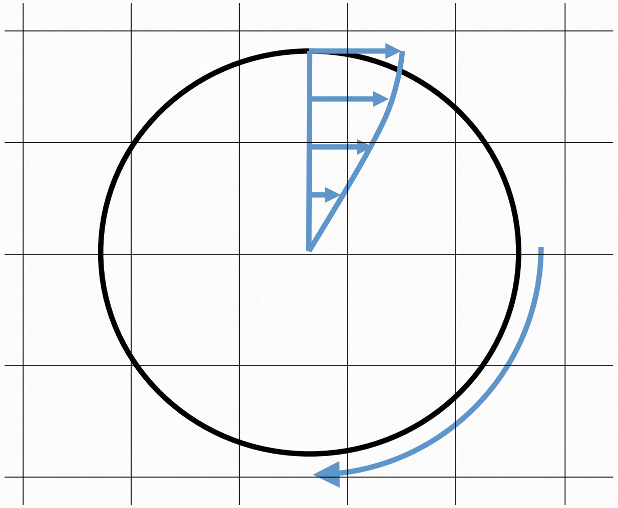

Exact solution:

$$u_\phi(r,t) = \frac{C}{J_1\left(\sqrt{\frac{iw\rho}{\mu}}R\right)} J_1\left(\sqrt{\frac{iw\rho}{\mu}}r\right) e^{(-iwt)}$$

Mesh Size	With Extrapolation 2nd order	Without Extrap. 1st order
0.05	0.1338	2.548
0.025	4.143 * 10^-2	0.9565
0.0125	1.067 * 10^-2	0.4761
0.00625	3.422 * 10^-3	0.265
0.003125	9.576 *10^-4	0.1404
K	**1.78**	**1**

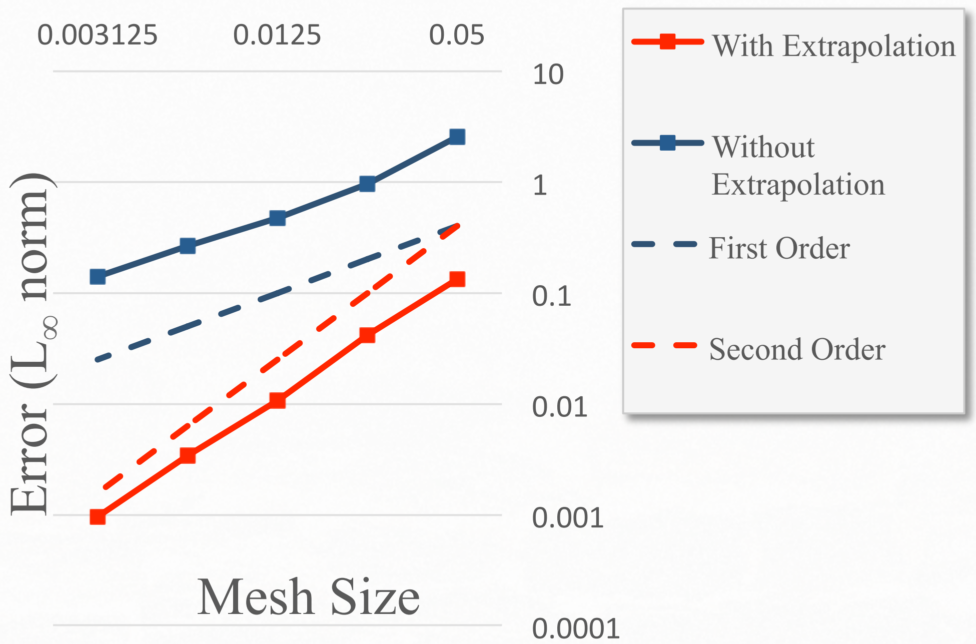

Turbulent Flows

Formulations based on turbulent viscosities:

Find $\boldsymbol{u} \in \boldsymbol{V}^h(\tilde{\Omega})$ *and* $p \in Q^h(\tilde{\Omega})$ *such that,* $\forall \boldsymbol{u} \in \boldsymbol{V}^h(\tilde{\Omega})$ *and* $\forall q \in Q^h(\tilde{\Omega})$,

$$0 = \mathbb{NS}[\mu + \mu_T](\boldsymbol{u}, p; \boldsymbol{w}, q) + \mathbb{STAB}[\mu + \mu_T](\boldsymbol{u}, p; \boldsymbol{w}, q)$$

- Spalart-Allmaras (SA) model with the Shifted Boundary Method are very similar to the Navier-Stokes equations
- Implicit LES is performed through the VMS stabilization/modeling approach

Wall model for the velocity boundary conditions:

$$\boldsymbol{u} = \boldsymbol{g} - \nabla \boldsymbol{u} \cdot \boldsymbol{d} \qquad \Rightarrow \qquad \boldsymbol{u} = \boldsymbol{g} - \boldsymbol{u}_{wall}(\boldsymbol{d}, \nabla \boldsymbol{u}, \dots)$$

$$u^+ = \frac{1}{\kappa} \log y^+ + C^+$$

$$u_\tau = \sqrt{\frac{\tau_w}{\rho}},$$

$$y^+ = \frac{u_\tau y}{\nu},$$

$$u^+ = \frac{u}{u_\tau},$$

Duke UNIVERSITY

Flow Over a Circular Cylinder

A classical test to validate algorithms for laminar/turbulent flow

Re	St (vs. reference)	C_D (vs. reference)	Reference source
20	-	2.09 (1.99)	[7]
100	0.167 (0.164,0.157)	1.35 (1.34)	[7, 39]
300	0.211 (0.203, 0.215)	1.38 (1.37)	[39]
3900	0.203 (0.203)	1.04 (1.00)	[7]

[7] Beaudan & Moin (1995)

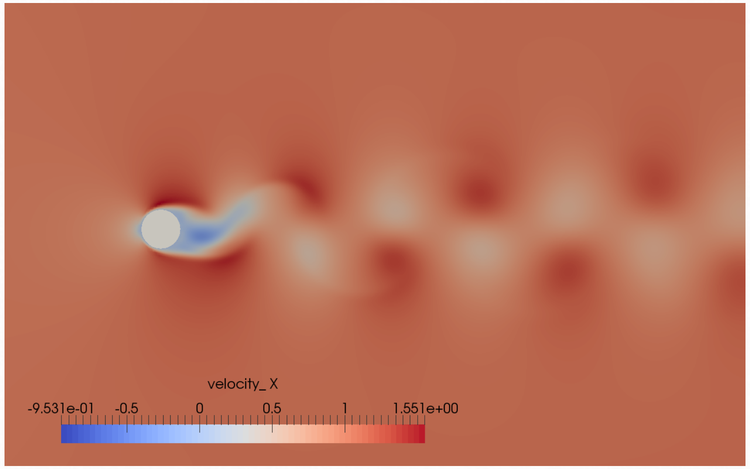

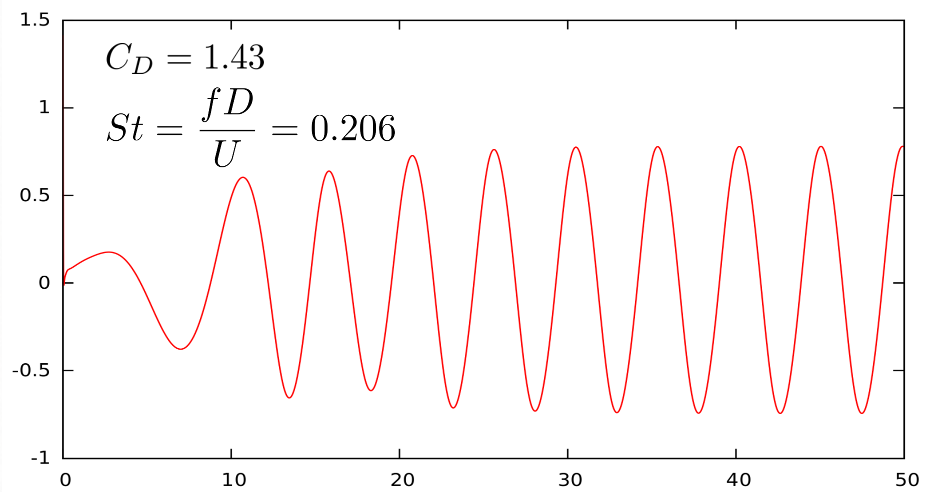

Lift coefficient, Re = 250

Flow Over a Circular Cylinder at Re=3,900

A classical test to validate algorithms for turbulent flow simulation

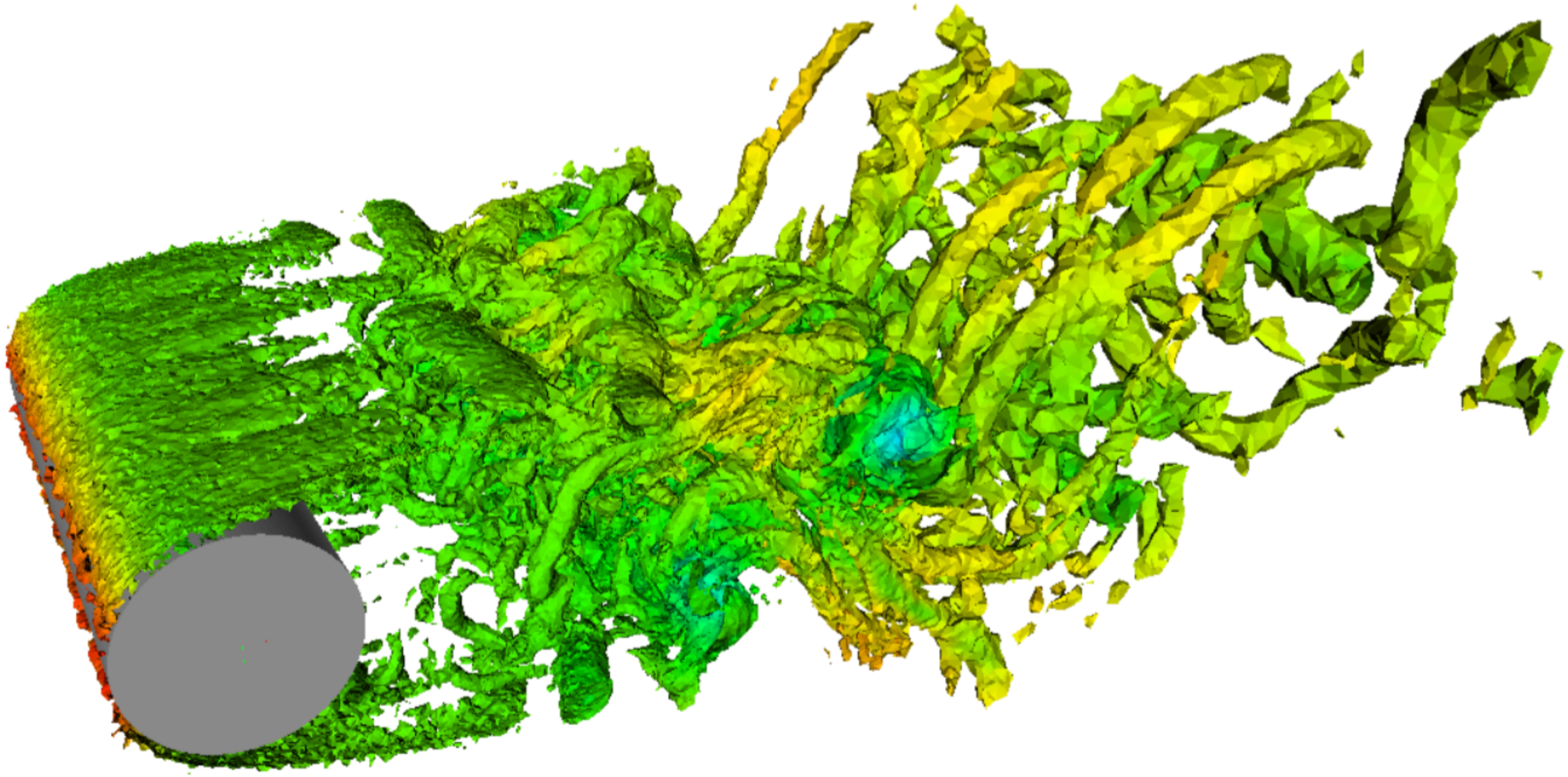

Q-criterion isosurfaces (used to visualize vortex structures)

Duke UNIVERSITY

Flow Over a Circular Cylinder at Re=3,900

A classical test to validate algorithms for turbulent flow simulation

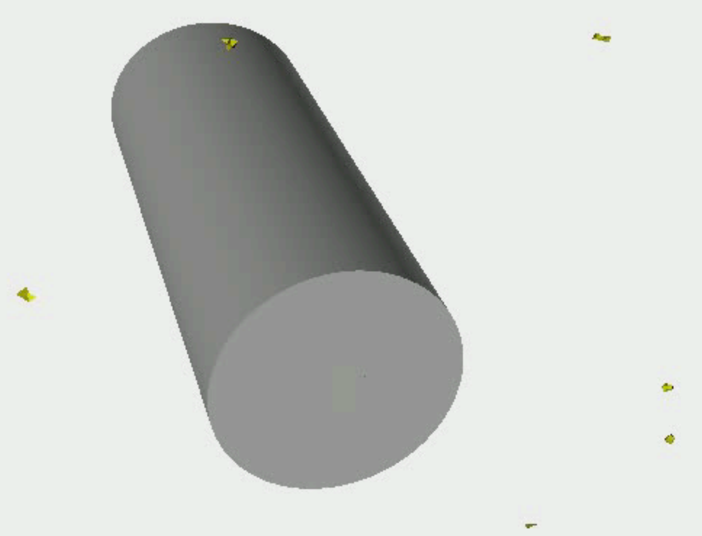

Q-criterion isosurfaces (used to visualize vortical structures)

A More Complicated Shape at Re=3,900

A differential geometry monster (the Monkey Trefoil)

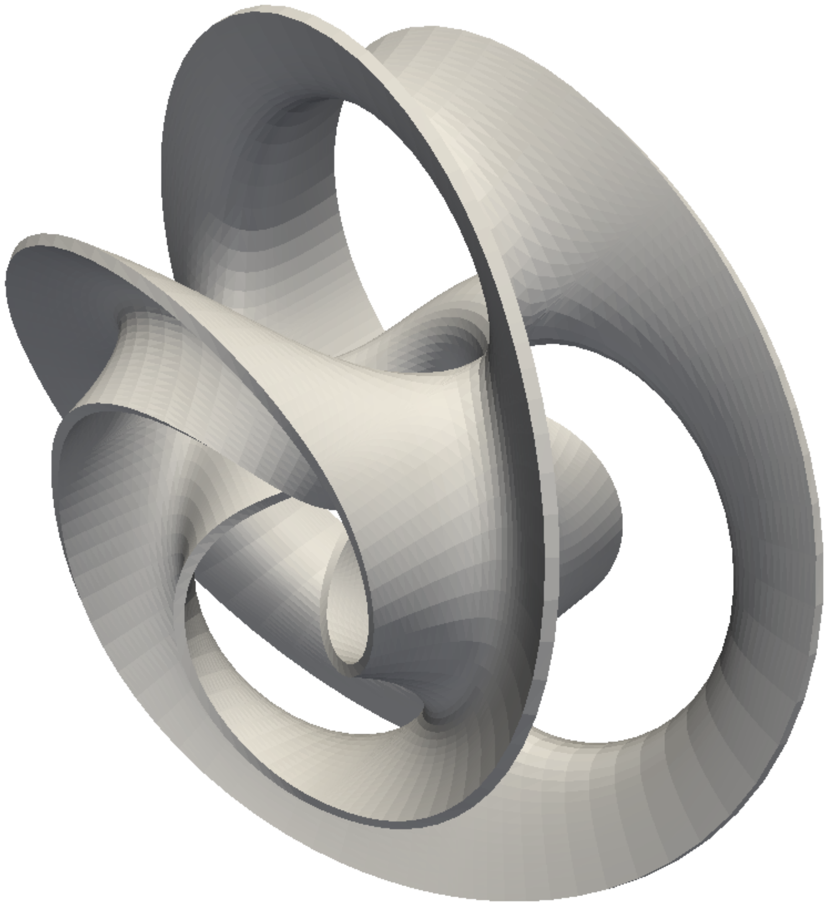

Duke UNIVERSITY

A More Complicated Shape at Re=3,900

A differential geometry monster (the Monkey Trefoil)

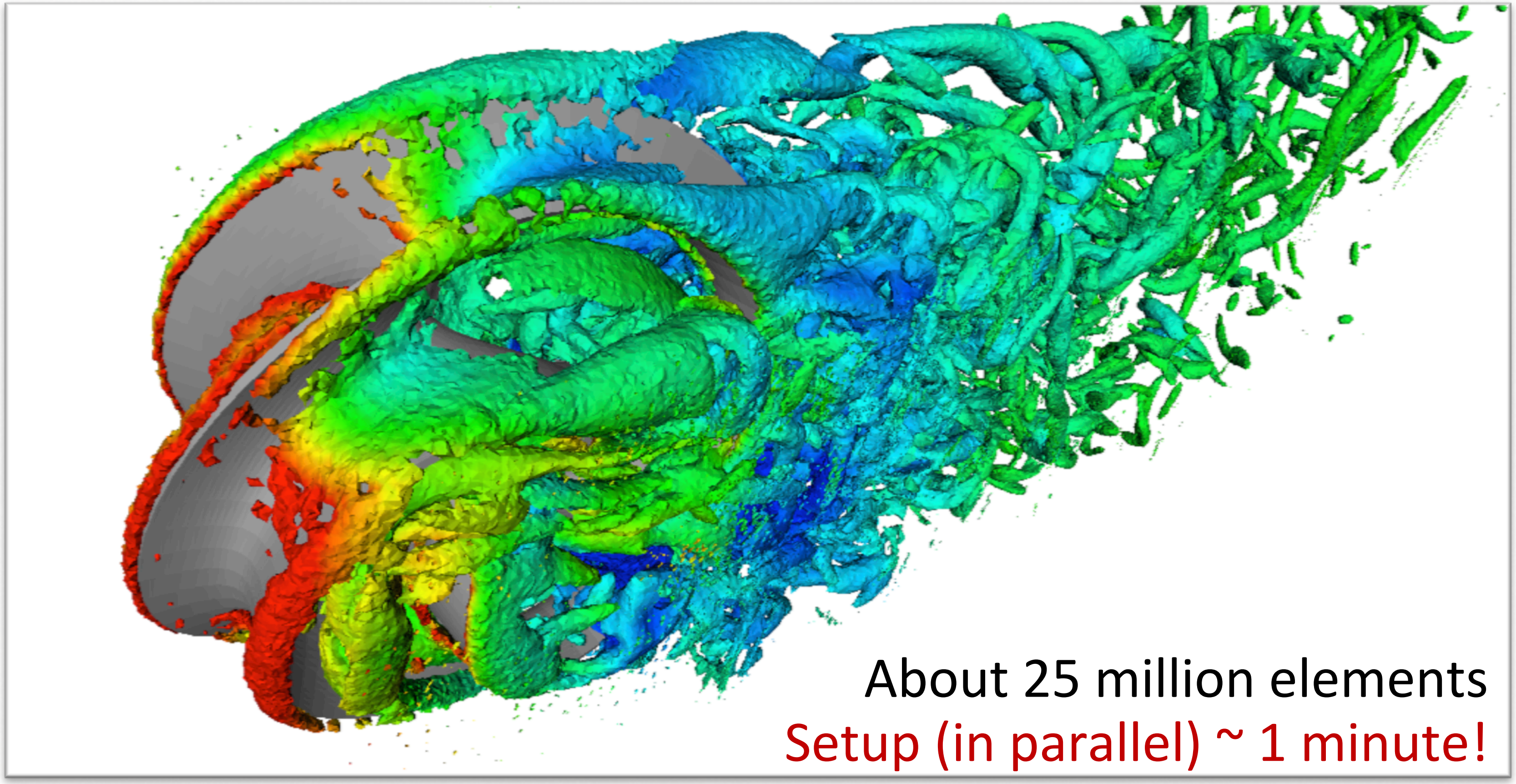

Q-criterion isosurfaces (used to visualize vortical structures)

Porous Media Flow (Mixed Formulation)

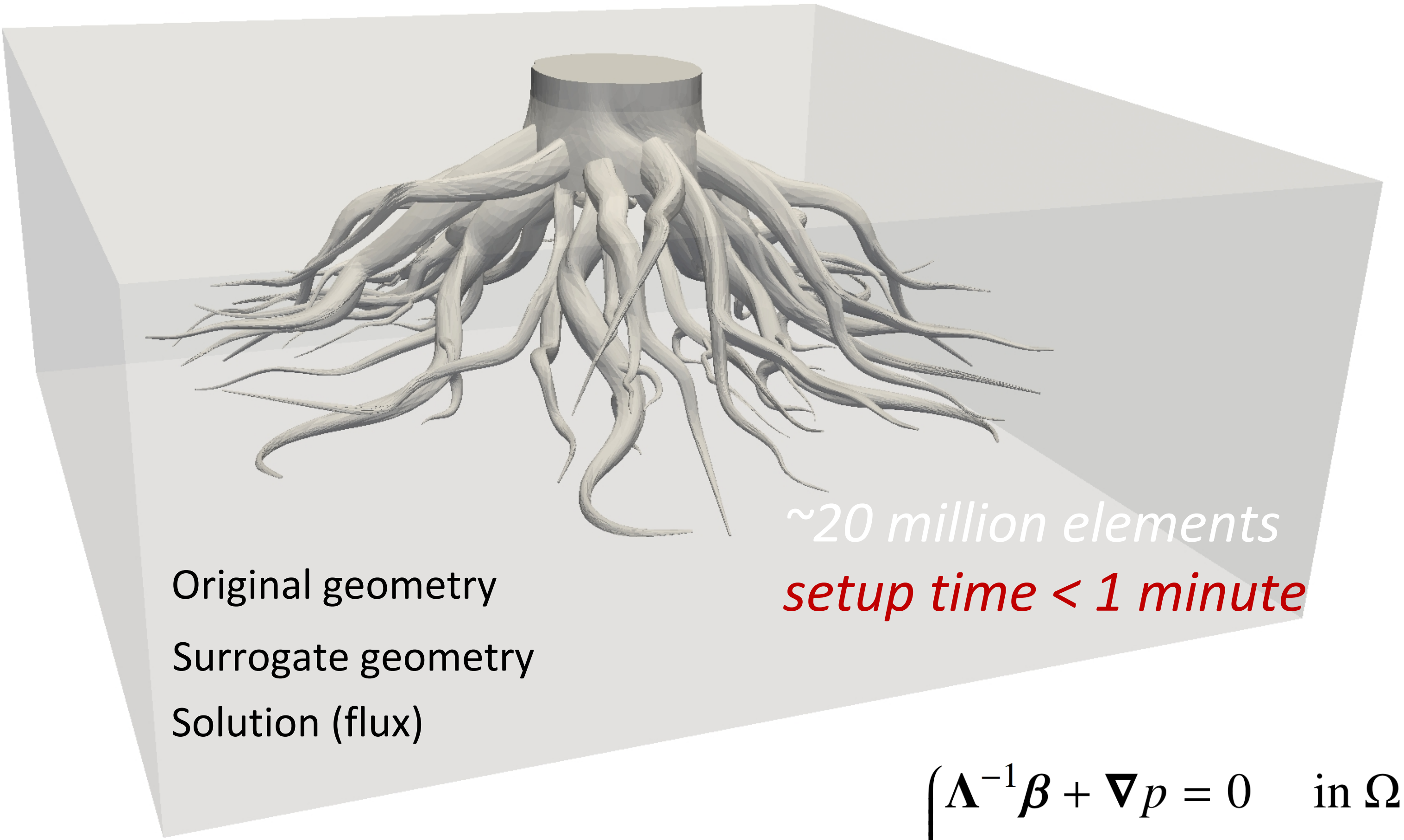

$$
\begin{cases}
\boldsymbol{\Lambda}^{-1}\boldsymbol{\beta} + \boldsymbol{\nabla} p = 0 & \text{in } \Omega \\
\boldsymbol{\nabla} \cdot \boldsymbol{\beta} = \phi & \text{in } \Omega \\
p = p_D & \text{on } \Gamma_D \\
\boldsymbol{\beta} \cdot \boldsymbol{n} = h_N & \text{on } \Gamma_N
\end{cases}
$$

Shifted *Interface* Method (Mixed Form)

A general (mixed) framework (Darcy-like):

$$\nabla \cdot \boldsymbol{\beta} = f \,, \qquad \boldsymbol{\beta} = -\kappa \nabla u \,,$$

$$[\![u]\!] = J_1 \,, \qquad [\![\boldsymbol{\beta}]\!] \cdot \boldsymbol{n} = -J_2 \,,$$

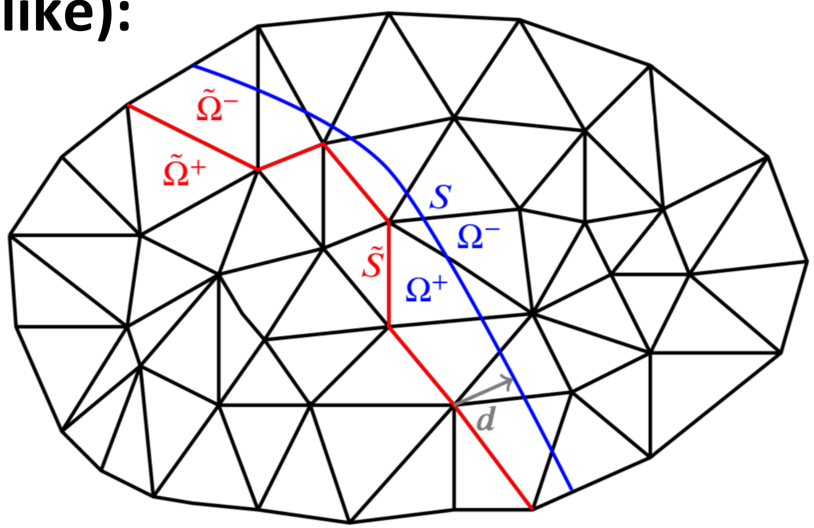

Taylor prolongation operators:

$$J_1 = [\![u + \nabla u \cdot \boldsymbol{d}]\!] + O\left(\|\boldsymbol{d}(\tilde{\boldsymbol{x}})\|^2\right) \,,$$

$$J_2 = -[\![\boldsymbol{\beta} + \nabla \boldsymbol{\beta} \boldsymbol{d}]\!] \cdot \boldsymbol{n} + O\left(\|\boldsymbol{d}(\tilde{\boldsymbol{x}})\|^2\right) \,.$$

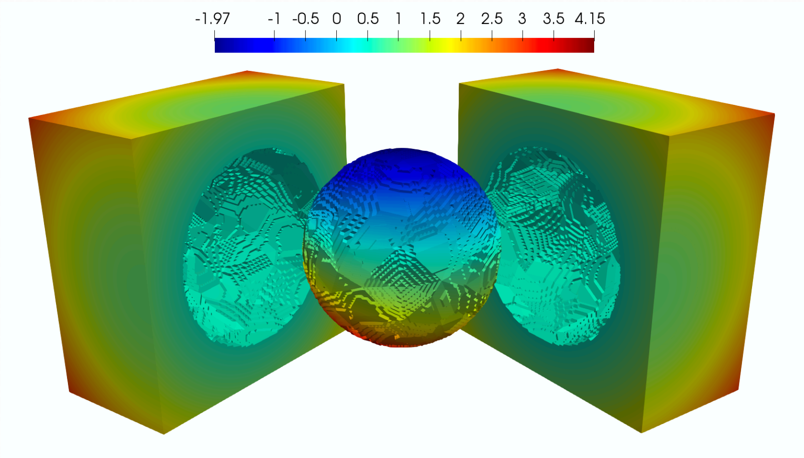

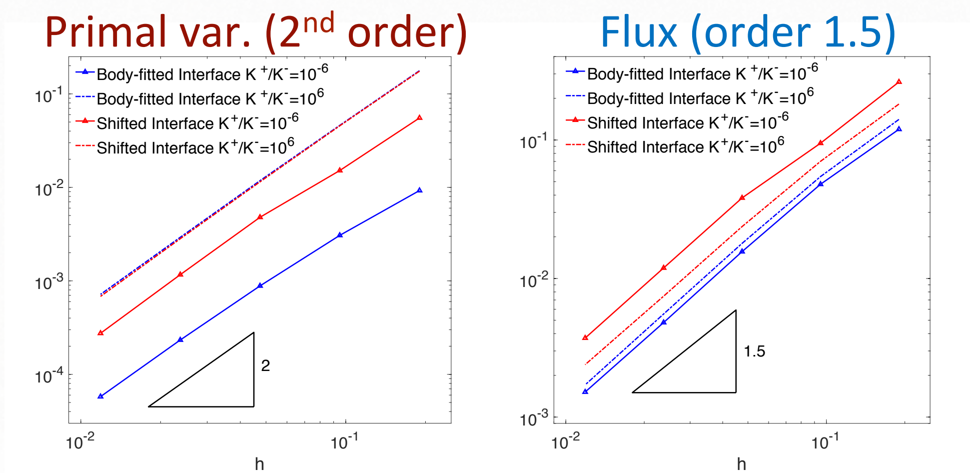

Shifted *Interface* Method (Mixed Form)

Three-dimensional numerical examples: Complex geometry

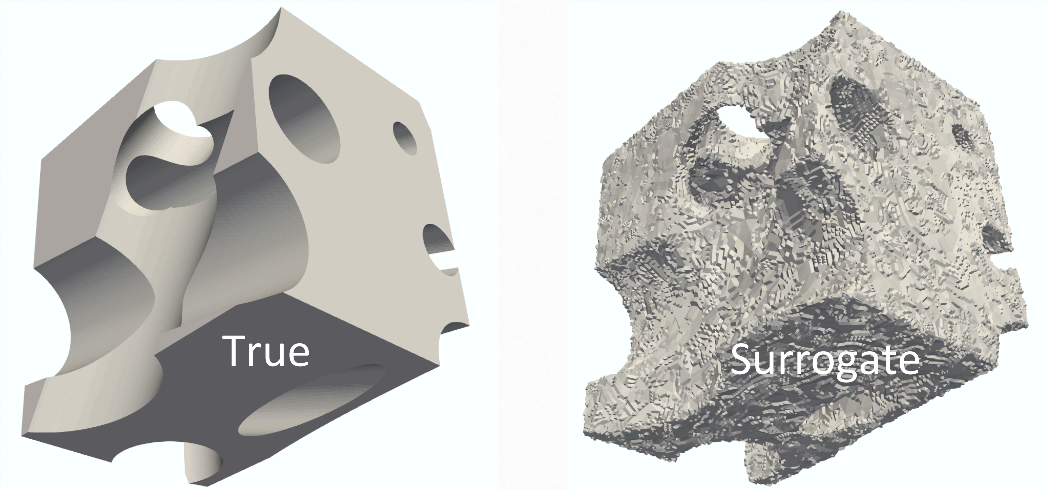

- Diffusivity ratio = 1000
- Manufactured solution
- Finest mesh: 23 million el.
- Setup time < 1 minute
- primary variable 2^{nd} – order accurate
- Flux variable accuracy of order 3/2

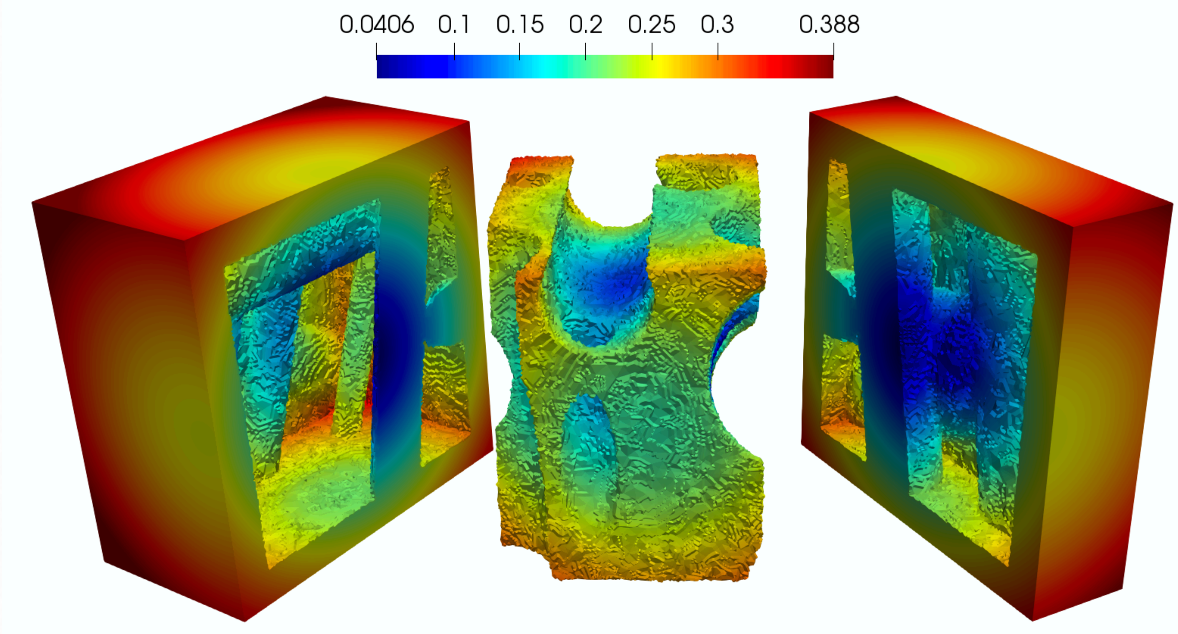

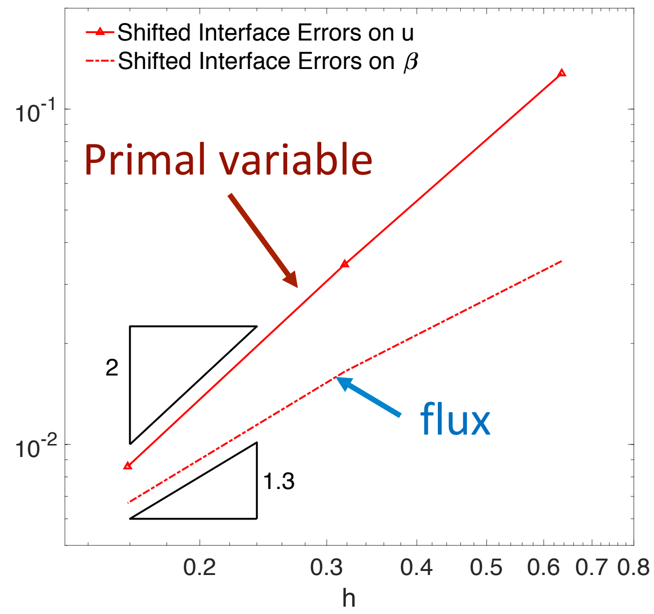

Static Linear Elasticity

Shifted boundary formulation for static linear elasticity (work with N. Atallah)

Base Nitsche method:

$$\int_\Omega \sigma^u_{ij} w_{i,j} - \int_\Gamma \sigma^u_{ij} w_i n_j - \int_\Gamma \sigma^w_{ij} n_j (u_i - g_i) + \int_\Gamma \kappa \frac{\gamma_\kappa}{h} ((n \otimes n)(u_i - g_i))(w_i) + \int_\Gamma \mu \frac{\gamma_\mu}{h} ((I - (n \otimes n))(u_i - g_i))(w_i) = \int_\Omega b_i w_i$$

Shifted Nitsche method:

$$\int_{\tilde\Omega} \sigma^u_{ij} w_{i,j} - \int_{\tilde\Gamma} \sigma^u_{ij} w_i n_j - \int_{\tilde\Gamma} \sigma^w_{ij} n_j (u_i + u_{i,k} d_k - g_i) + \int_{\tilde\Gamma} \kappa \frac{\gamma_\kappa}{h} ((n \otimes n)(u_i + u_{i,k} d_k) - g_i)(w_i + w_{i,k} d_k) + \int_{\tilde\Gamma} \mu \frac{\gamma_\mu}{h} ((I - (n \otimes n))(u_i + u_{i,k} d_k) - g_i)(w_i + w_{i,k} d_k) = \int_{\tilde\Omega} b_i w_i$$

Static Linear Elasticity

Problem Statement

- Domain (Ω): Unit square
- Zero Dirichlet boundary condition on Γ

Exact Solution:

$$\begin{bmatrix} C\sin(\pi x)\sin(\pi y) \\ C\sin(\pi x)\sin(\pi y) \end{bmatrix}$$

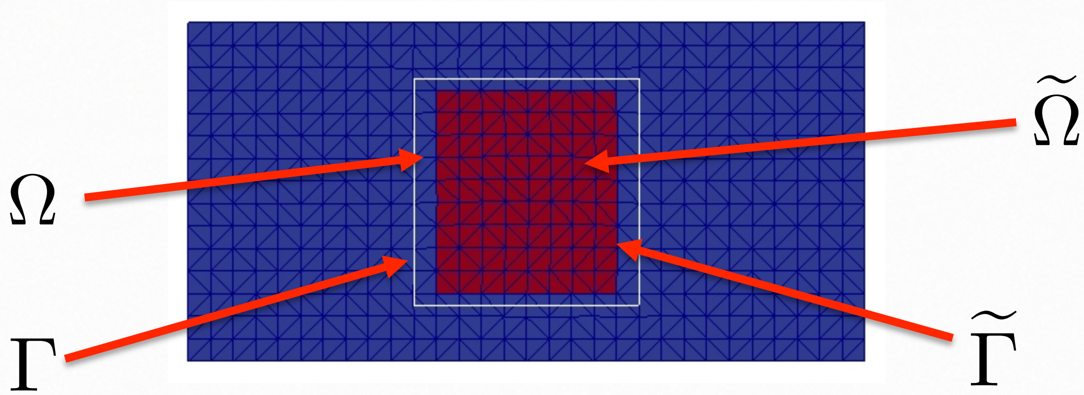

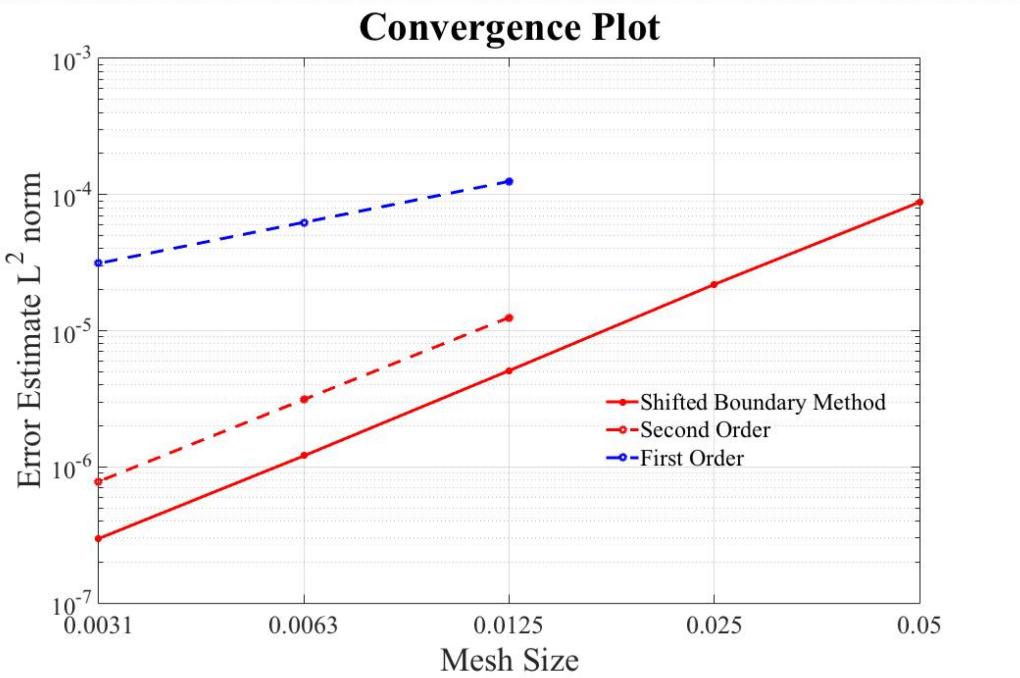

The Shifted Boundary Method in Action

Example: A linearly elastic compressible solid

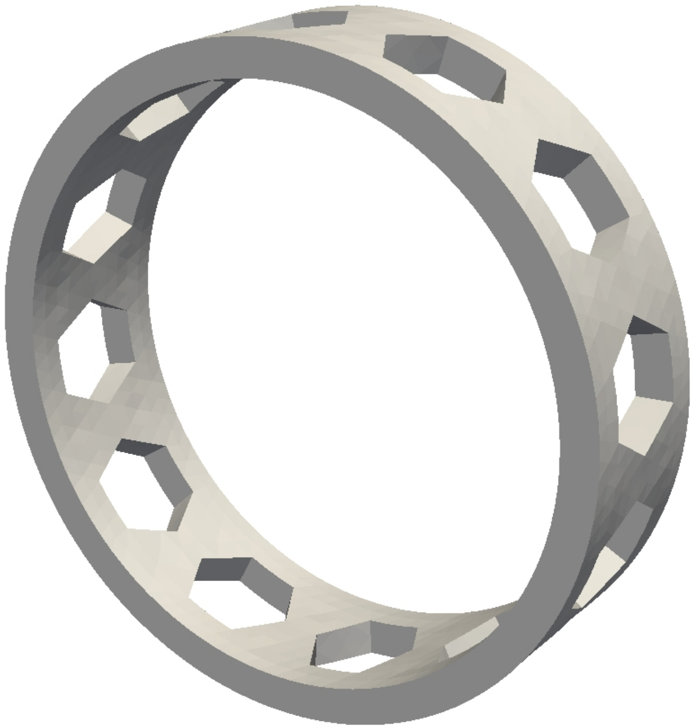

Original geometry

The Shifted Boundary Method in Action

Example: A linearly elastic compressible solid

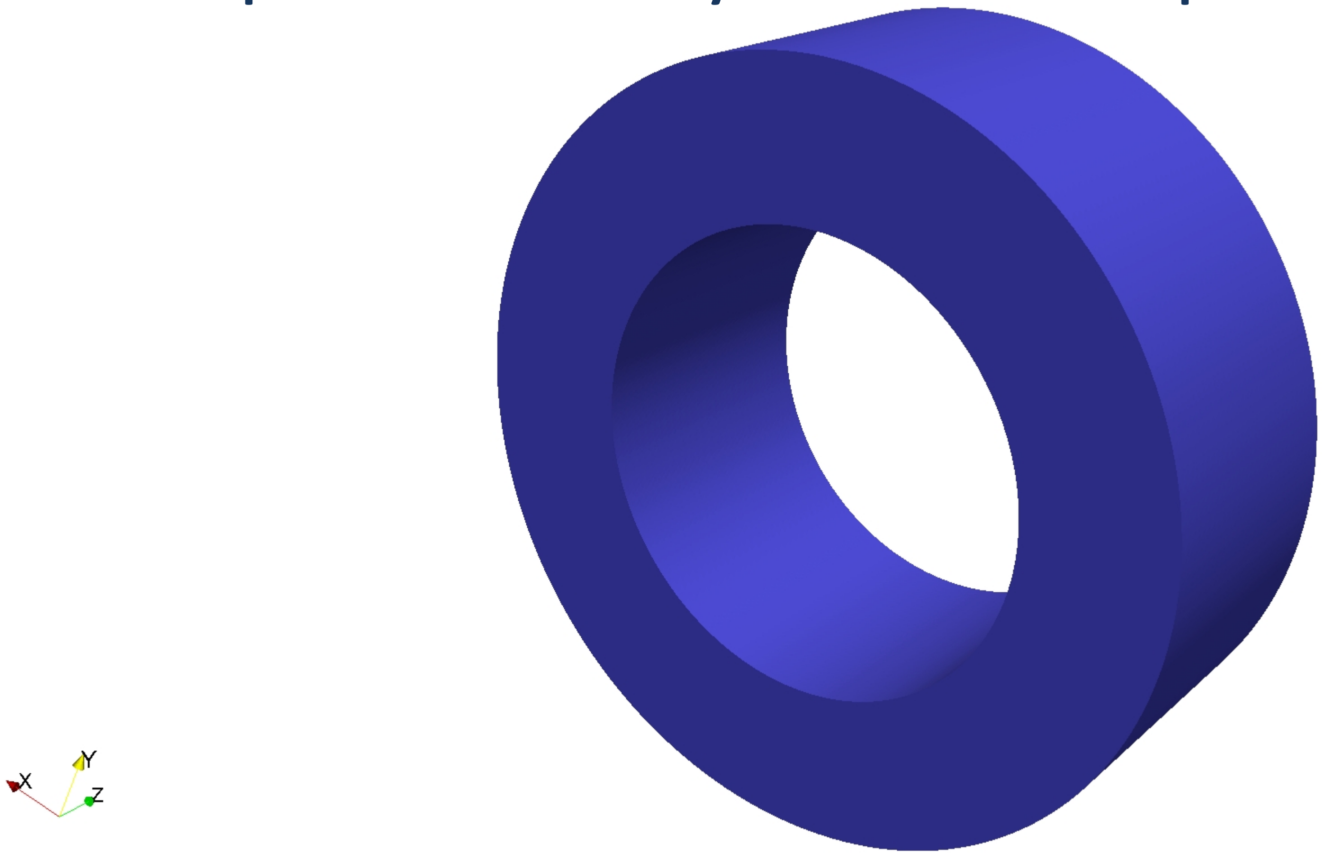

The background domain

The Shifted Boundary Method in Action

Example: A linearly elastic compressible solid

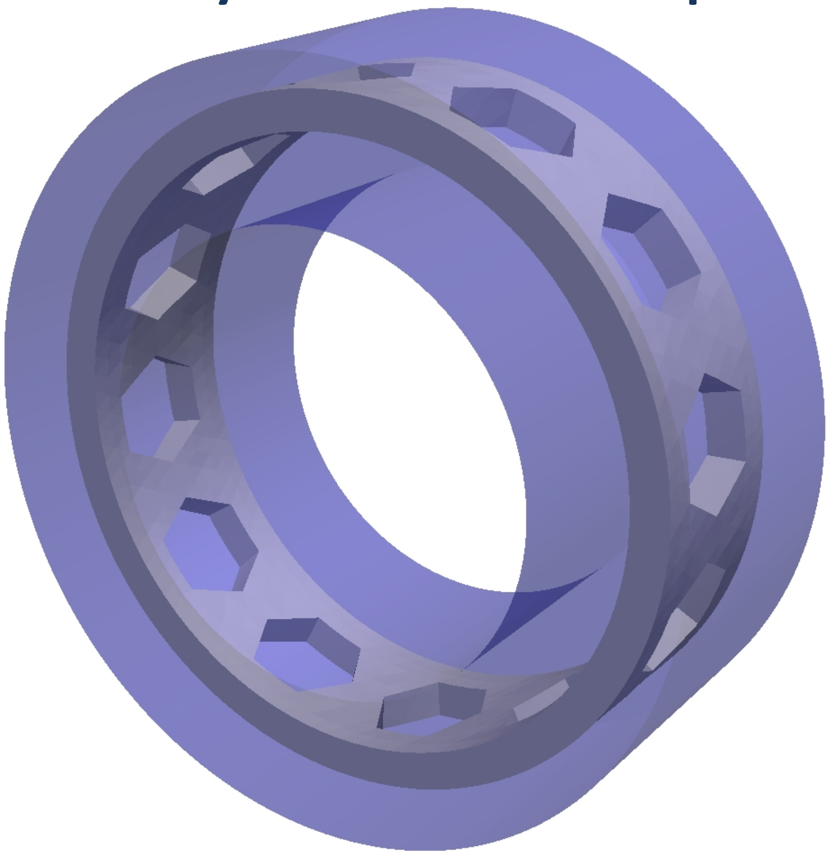

The background domain and the immersed original geometry

The Shifted Boundary Method in Action

Example: A linearly elastic compressible solid

The initial set of active elements (with boundary conditions sidesets)

The Shifted Boundary Method in Action

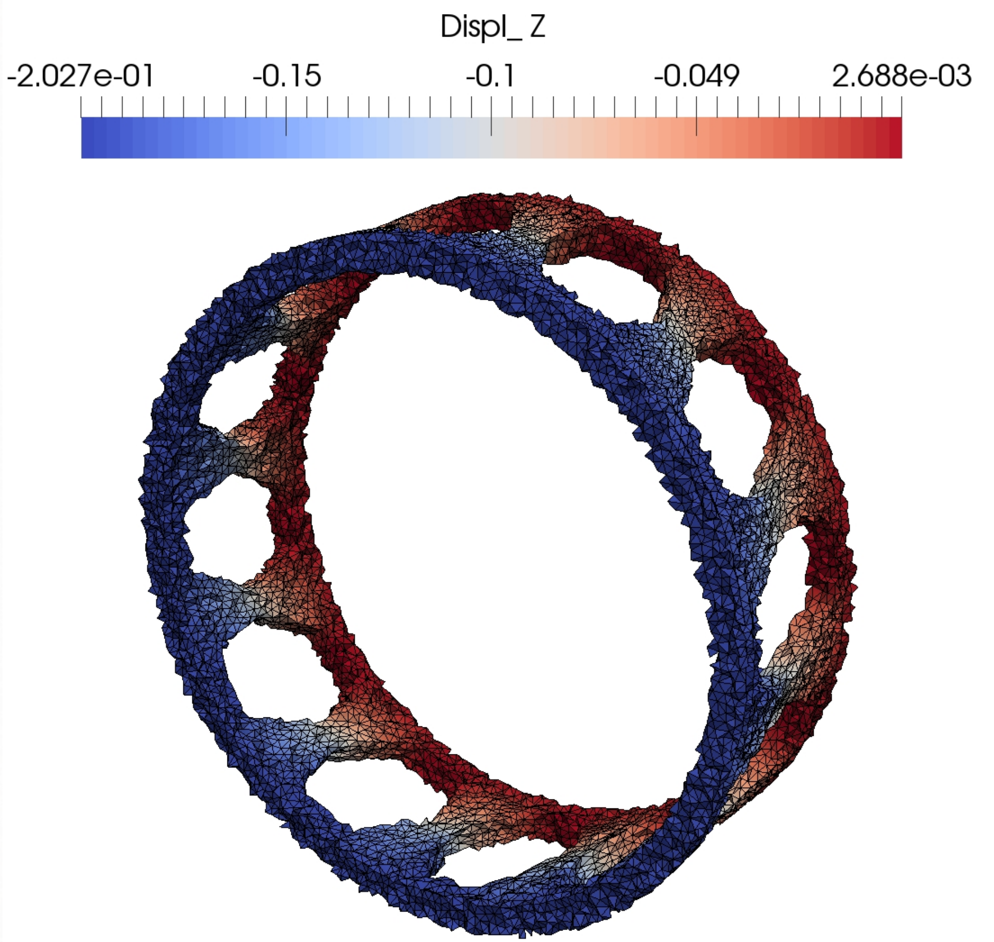

Deformed configuration of the set of active elements

The Shifted Boundary Method in Action

The intersection of the immersed geometry with the grid

The Shifted Boundary Method in Action

Deformation of the intersected immersed geometry

Static Linear Elasticity: 3D cylinder

Problem Statement:

- Domain (Ω): Stent (r = 1.8, L =14.4).
- Zero forcing term

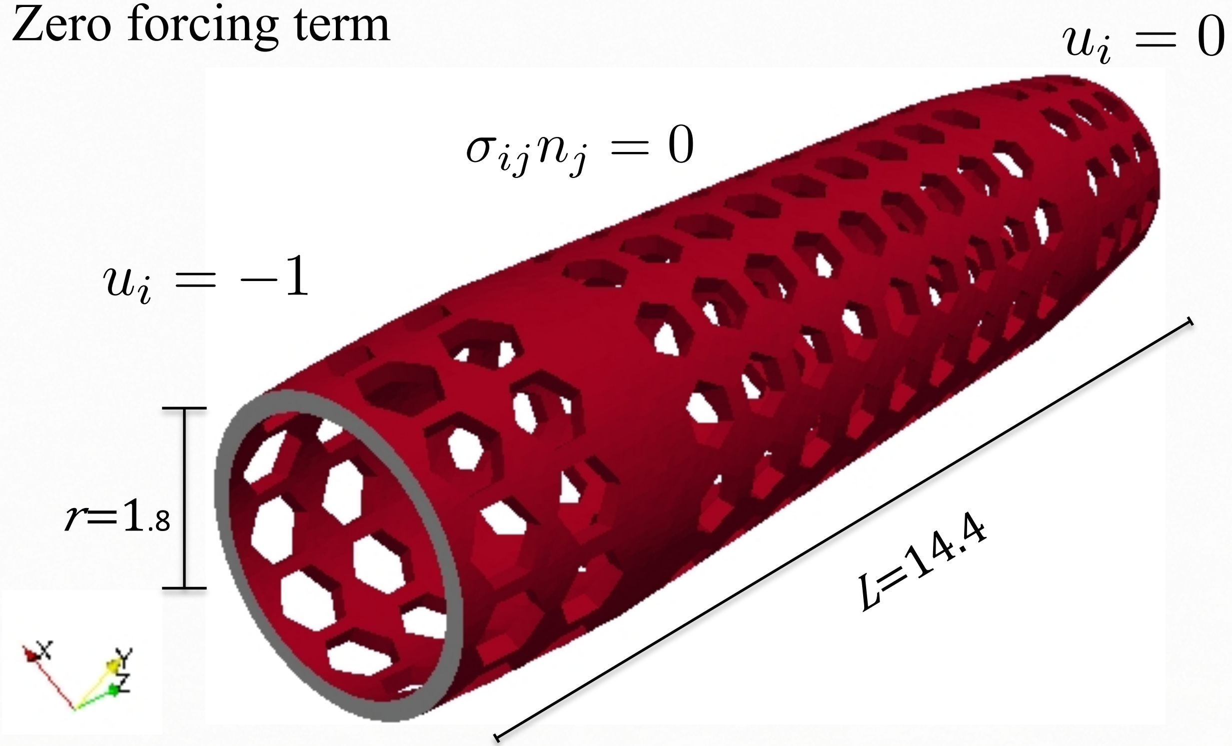

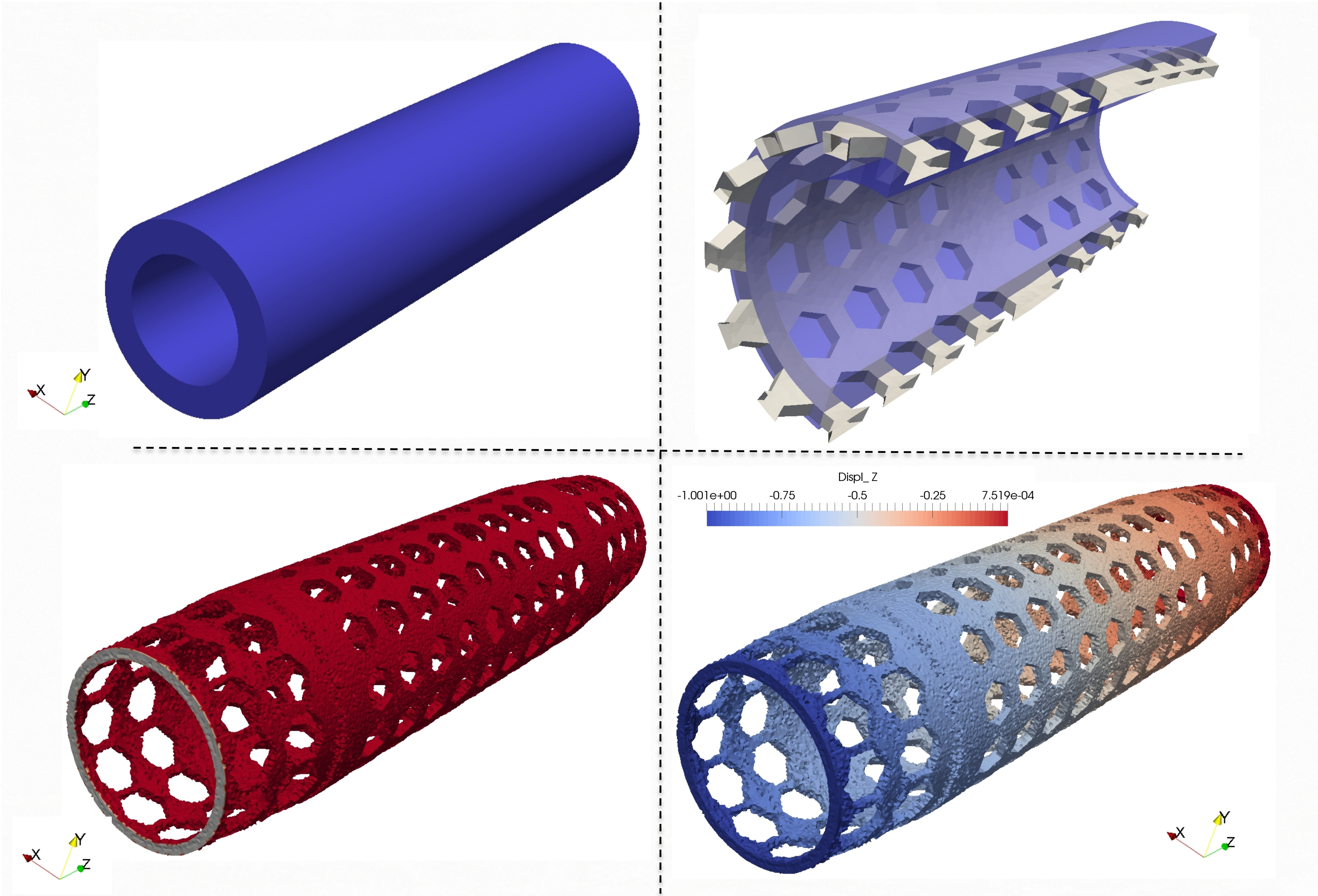

Duke UNIVERSITY

Acknowledgments & Future Directions

Ongoing work [contact guglielmo.scovazzi@duke.edu for drafts]

- **Numerical analysis of SBM for Stokes and Darcy operators** *(collaboration with C. Canuto)*
- **High-order approximations** *(collaborators: M. Ricchiuto & C. Canuto)*
- **CFD + ROM** *(collaboration with E. Karatzas, G. Stabile, G. Rozza)*
- **Free surface flows and multiphase flows**

Development of the *shifted boundary method* was supported by:

- PECASE Award (Executive Office of the White House, USA)
- DOE Early Career Award (ASCR) [mathematical framework]
- ONR [Navier-Stokes, free surface flows, acoustics, shallow water flows]
- ARO [solid mechanics]
- ExxonMobil Upstream Research Company [mechanics & geomechanics]

Duke UNIVERSITY